IMAGE RESTORATION AND RECONSTRUCTION

- 5.1 A Model of Image Degradation/Restoration Process
- 5.2 Noise Model
- 5.3 Restoration in the Presence of Noise Only - Spatial Filtering
- 5.4 Periodic Noise Reduction by Frequency Domain Filtering
- 5.5 Linear, Position-Invariant Degradations

Prof. Ta-Te Lin
Dept. of Biomechatroincs Engineering, National Taiwan University

IMAGE RESTORATION AND RECONSTRUCTION

- 5.6 Estimating the Degradation Function
- 5.7 Inverse Filtering
- 5.8 Minimum Mean Square Error (Wiener) Filtering
- 5.9 Constrained Least Squares Filtering
- 5.10 Geometric Mean Filter
- 5.11 Image Reconstruction From Projections

Prof. Ta-Te Lin
Dept. of Biomechatroincs Engineering, National Taiwan University

5.1 A Model of Image Degradation / Restoration Process

- Degradation in spatial domain

$$g(x,y) = h(x,y) \star f(x,y) + \eta(x,y) \qquad (5\text{-}1)$$

- Degradation in frequency domain

$$G(u,v) = H(u,v)F(u,v) + N(u,v) \qquad (5\text{-}2)$$

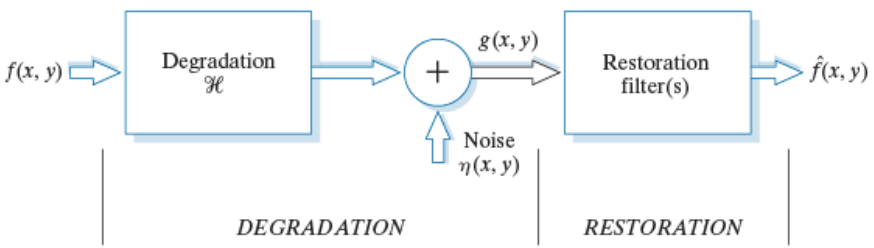

FIGURE 5.1 A model of the image degradation/ restoration process.

5.2 Noise Model

5.2.1 Spatial and Frequency Properties of Noise

- White Noise
  - Fourier spectrum is a constant
- Assume that the noise is independent of the space coordinates and is a random noise.
- Describe the noise in probability mode

5.2 Noise Model

5.2.2 Some Important Noise Probability Density Functions

- Gaussian Noise

$$p(z) = \frac{1}{\sqrt{2\pi}\sigma} e^{-(z-\mu)^2/2\sigma^2} \qquad (5-3)$$

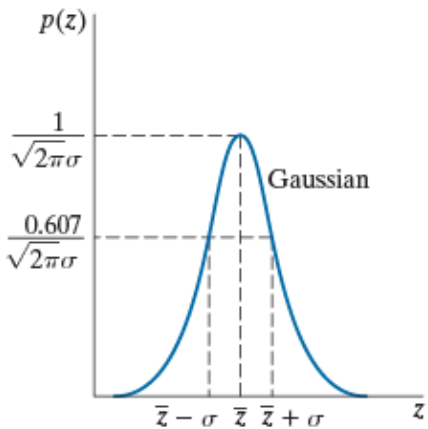

5.2 Noise Model

5.2.2 Some Important Noise Probability Density Functions

- Rayleigh Noise

$$p(z) = \begin{cases} \frac{2}{b}(z-a)e^{-(z-a)^2/b} & \text{for } z \geq a \\ 0 & \text{for } z < a \end{cases} \qquad (5\text{-}4)$$

mean : $\mu = a + \sqrt{\pi b/4}$ (5-5)

variance : $\sigma^2 = \frac{b(4-\pi)}{4}$ (5-6)

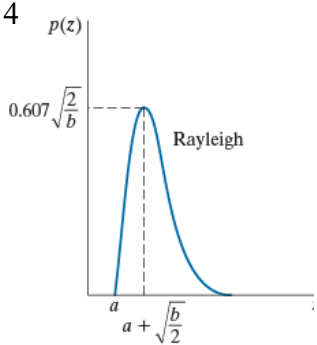

5.2 Noise Model

5.2.2 Some Important Noise Probability Density Functions

- Erlang (Gamma) Noise

$$p(z) = \begin{cases} \dfrac{a^b z^{b-1}}{(b-1)!} e^{-az} & \text{for } z \geq 0 \\ 0 & \text{for } z < 0 \end{cases} \qquad (5\text{-}7)$$

$$\text{mean}: \quad \bar{z} = \frac{b}{a} \qquad (5\text{-}8)$$

$$\text{variance}: \quad \sigma^2 = \frac{b}{a^2} \qquad (5\text{-}9)$$

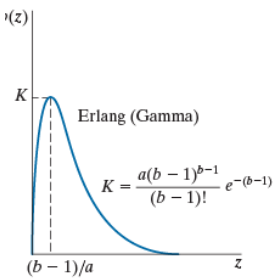

5.2 Noise Model

5.2.2 Some Important Noise Probability Density Functions

- Exponential Noise

$$p(z) = \begin{cases} ae^{-az} & \text{for } z \geq 0 \\ 0 & \text{for } z < 0 \end{cases} \qquad (5\text{-}10)$$

mean : $\bar{z} = \frac{1}{a}$ (5-11)

variance : $\sigma^2 = \frac{1}{a^2}$ (5-12)

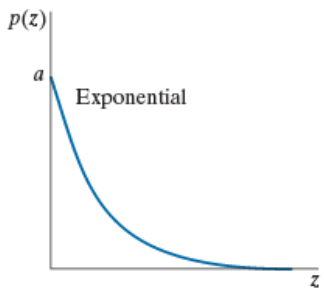

5.2 Noise Model

5.2.2 Some Important Noise Probability Density Functions

- Uniform Noise

$$p(z) = \begin{cases} \dfrac{1}{(b-a)} & \text{if } a \le z \le b \\ 0 & \text{otherwise} \end{cases} \qquad (5\text{-}13)$$

$$\text{mean}: \quad \bar{z} = \frac{a+b}{2} \qquad (5\text{-}14)$$

$$\text{variance}: \quad \sigma^2 = \frac{(b-a)^2}{12} \qquad (5\text{-}15)$$

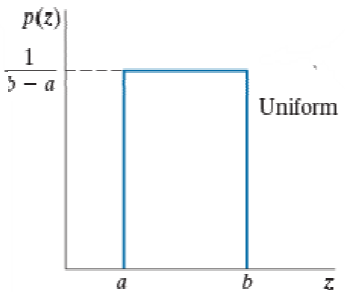

5.2 Noise Model

5.2.2 Some Important Noise Probability Density Functions

- Impulse, Salt-and-pepper Noise

$$p(z) = \begin{cases} P_a & \text{for } z = a \\ P_b & \text{for } z = b \\ 0 & \text{otherwise} \end{cases} \qquad (5\text{-}16)$$

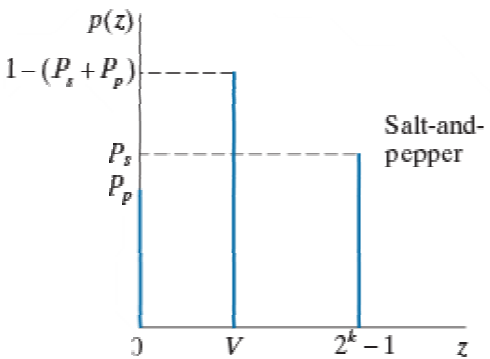

5.2 Noise Model

5.2.2 Some Important Noise Probability Density Functions

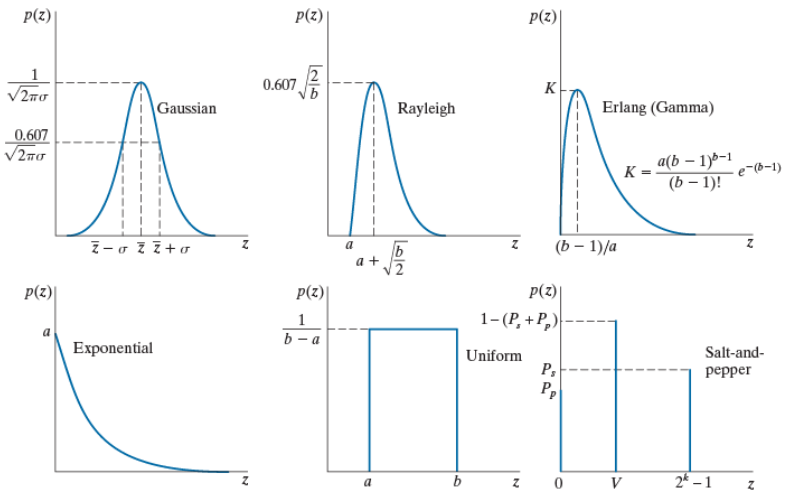

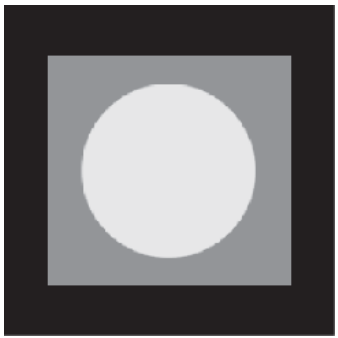

FIGURE 5.3
Test pattern used to illustrate the characteristics of the PDFs from Fig. 5.2.

5.2 Noise Model

5.2.2 Some Important Noise Probability Density Functions

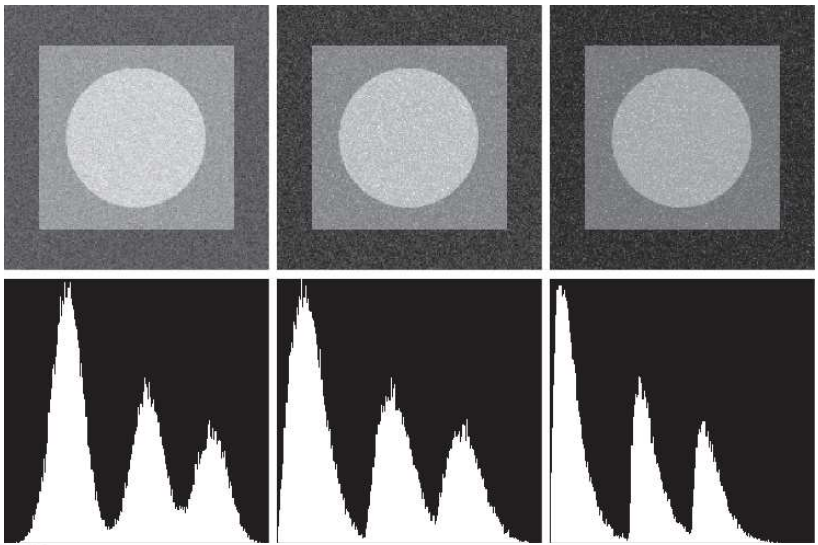

a b c
d e f

FIGURE 5.4 Images and histograms resulting from adding Gaussian, Rayleigh, and Erlanga noise to the image in Fig. 5.3.

5.2 Noise Model

5.2.2 Some Important Noise Probability Density Functions

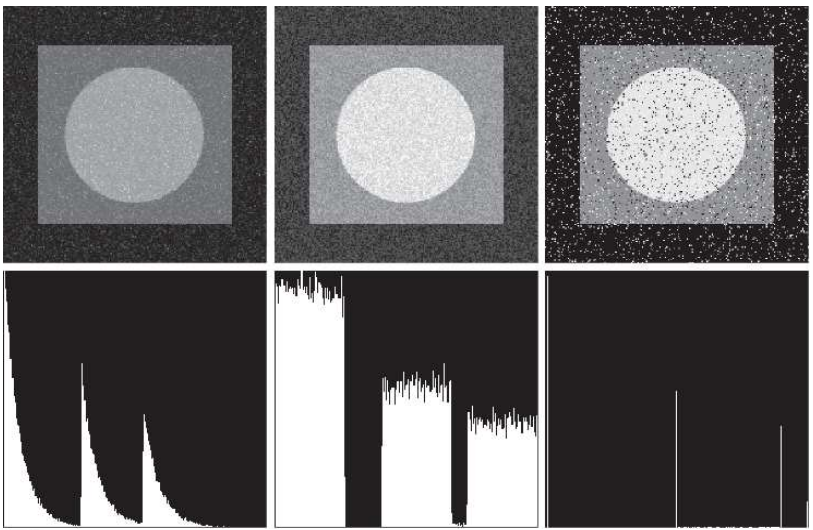

g h i
j k l

FIGURE 5.4 (*continued*) Images and histograms resulting from adding exponential, uniform, and salt-and-pepper noise to the image in Fig. 5.3. In the salt-and-pepper histogram, the peaks in the origin (zero intensity) and at the far end of the scale are shown displaced slightly so that they do not blend with the page background.

5.2 Noise Model

5.2.3 Periodic Noise

- Space-related noise
- Can usually be processed using frequency domain filtering

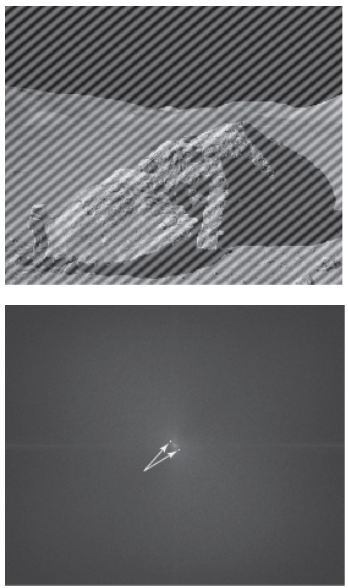

a b

FIGURE 5.5
(a) Image corrupted by additive sinusoidal noise. (b) Spectrum showing two conjugate impulses caused by the sine wave. (Original image courtesy of NASA.)

5.2 Noise Model

5.2.4 Estimation of Noise Parameters

- Evaluated by sensor characteristics or specifications
- Apply the average and standard deviation of the statistical distribution to estimate noise parameters

$$\bar{z} = \sum_{i=0}^{L-1} z_i p_S(z_i) \qquad (5\text{-}19)$$

$$\sigma^2 = \sum_{i=0}^{L-1} (z_i - \bar{z})^2 p_S(z_i) \qquad (5\text{-}20)$$

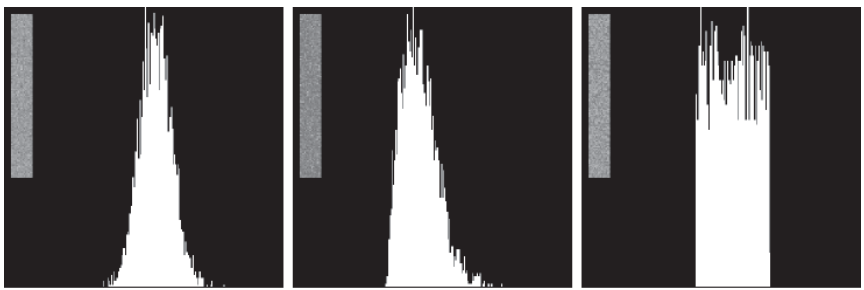

a b c

FIGURE 5.6 Histograms computed using small strips (shown as inserts) from (a) the Gaussian, (b) the Rayleigh, and (c) the uniform noisy images in Fig. 5.4.

5.3 Restoration in the Presence of Noise Only—Spatial Filtering

- Assume that the only factor that causes image attenuation is noise

$$g(x,y) = f(x,y) + \eta(x,y) \qquad (5\text{-}21)$$

$$G(u,v) = F(u,v) + N(u,v) \qquad (5\text{-}22)$$

- Known noise and unknown noise processing methods

5.3 Restoration in the Presence of Noise Only—Spatial Filtering

5.3.1 Mean Filters

- Arithmetic Mean Filter

$$\hat{f}(x,y)=\frac{1}{mn}\sum_{(s,t)\in S_{xy}} g(x,y) \qquad (5-23)$$

- Geometric Mean Filter

$$\hat{f}(x,y)=\left[\prod_{(s,t)\in S_{xy}} g(x,y)\right]^{\frac{1}{mn}} \qquad (5-24)$$

- Harmonic Mean Filter

$$\hat{f}(x,y)=\frac{mn}{\sum_{(s,t)\in S_{xy}} \frac{1}{g(x,y)}} \qquad (5-25)$$

- Contraharmonic Mean Filter

$$\hat{f}(x,y)=\frac{\sum_{(s,t)\in S_{xy}} g(x,y)^{Q+1}}{\sum_{(s,t)\in S_{xy}} g(x,y)^{Q}} \qquad (5-26)$$

5.3 Restoration in the Presence of Noise Only—Spatial Filtering

5.3.1 Mean Filters

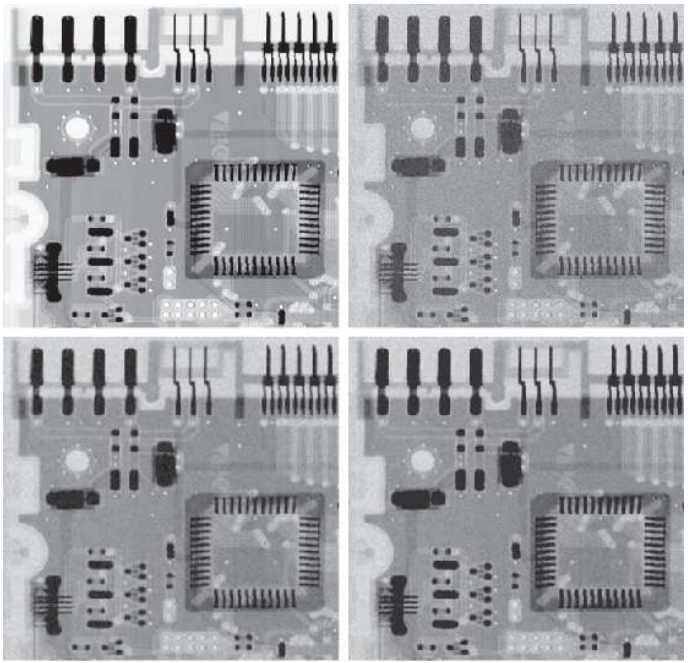

a b
c d

FIGURE 5.7
(a) X-ray image of circuit board. (b) Image corrupted by additive Gaussian noise. (c) Result of filtering with an arithmetic mean filter of size 3×3. (d) Result of filtering with a geometric mean filter of the same size. (Original image courtesy of Mr. Joseph E. Pascente, Lixi, Inc.)

5.3 Restoration in the Presence of Noise Only—Spatial Filtering

5.3.1 Mean Filters

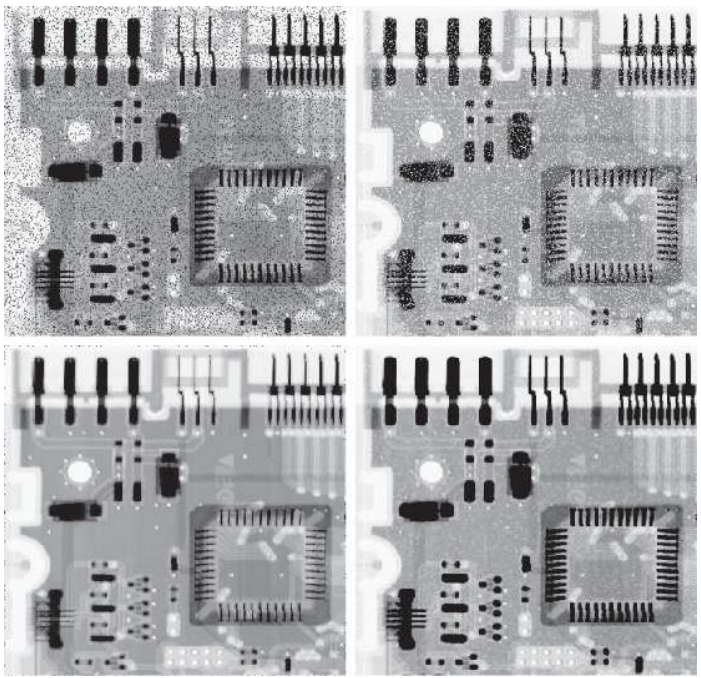

a b
c d

FIGURE 5.8
(a) Image corrupted by pepper noise with a probability of 0.1. (b) Image corrupted by salt noise with the same probability. (c) Result of filtering (a) with a 3×3 contra-harmonic filter $Q = 1.5$. (d) Result of filtering (b) with $Q = -1.5$.

5.3 Restoration in the Presence of Noise Only—Spatial Filtering

5.3.1 Mean Filters

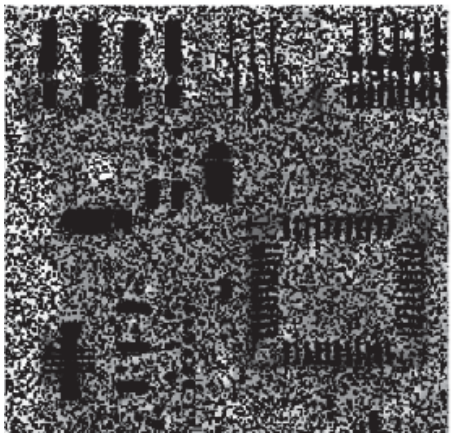

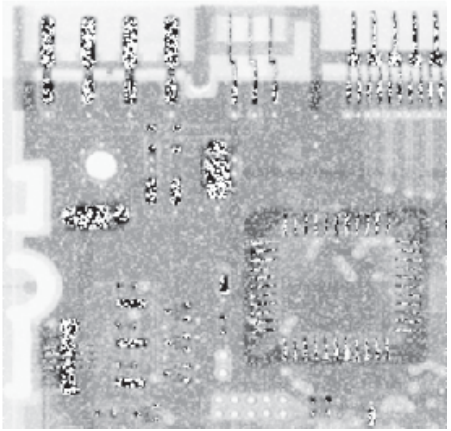

a b

FIGURE 5.9 Results of selecting the wrong sign in contraharmonic filtering. (a) Result of filtering Fig. 5.8(a) with a contraharmonic filter of size 3×3 and $Q = -1.5$. (b) Result of filtering Fig. 5.8(b) using $Q = 1.5$.

5.3 Restoration in the Presence of Noise Only—Spatial Filtering

5.3.2 Order-Statistic Filters

- Median Filter

$$\hat{f}(x,y) = \underset{(s,t)\in S_{xy}}{median}\{g(s,t)\} \qquad (5\text{ - }27)$$

- Max and Min Filters

$$\hat{f}(x,y) = \max_{(s,t)\in S_{xy}}\{g(s,t)\} \qquad (5\text{ - }28)$$

$$\hat{f}(x,y) = \min_{(s,t)\in S_{xy}}\{g(s,t)\} \qquad (5\text{ - }29)$$

- Midpoint Filters

$$\hat{f}(x,y) = \frac{1}{2}\left[\max_{(s,t)\in S_{xy}}\{g(s,t)\} + \min_{(s,t)\in S_{xy}}\{g(s,t)\}\right] \qquad (5\text{ - }30)$$

- Alpha-trimmed Mean Filter

$$\hat{f}(x,y) = \frac{1}{mn-d}\sum_{(s,t)\in S_{xy}} g_r(s,t) \qquad (5\text{ - }31)$$

5.3 Restoration in the Presence of Noise Only—Spatial Filtering

5.3.2 Order-Statistic Filters

a b
c d

FIGURE 5.10
(a) Image corrupted by salt-and- pepper noise with probabilities $P_s = P_p = 0.1$. (b) Result of one pass with a median filter of size 3×3. (c) Result of processing (b) with this filter. (d) Result of processing (c) with the same filter.

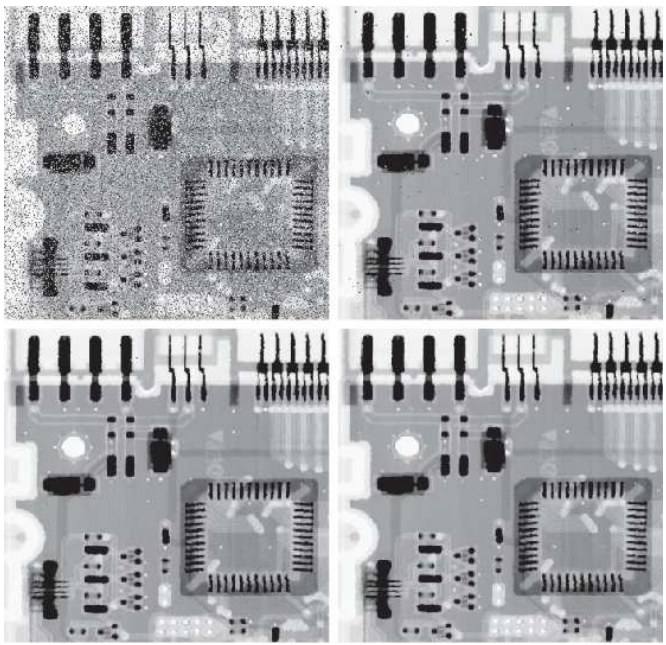

5.3 Restoration in the Presence of Noise Only—Spatial Filtering

5.3.2 Order-Statistic Filters

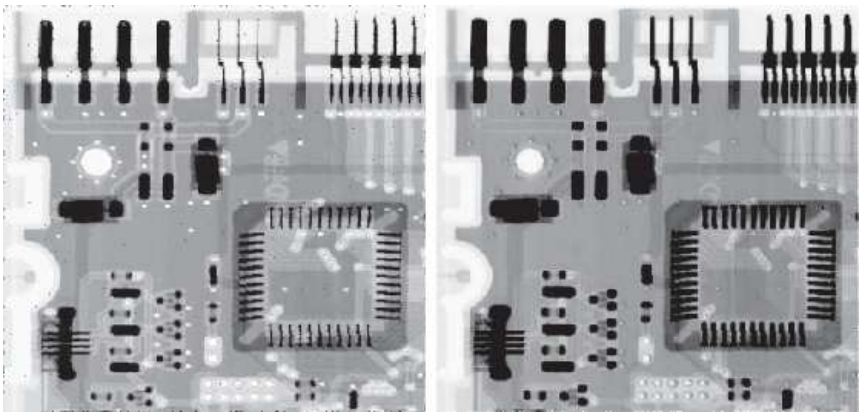

a b

FIGURE 5.11
(a) Result of filtering Fig. 5.8(a) with a max filter of size 3×3.
(b) Result of filtering Fig. 5.8(b) with a min filter of the same size.

5.3 Restoration in the Presence of Noise Only—Spatial Filtering

5.3.2 Order-Statistic Filters

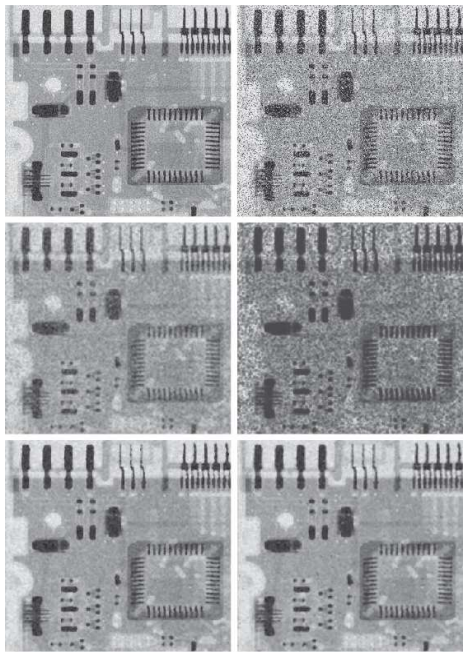

a b
c d
e f

FIGURE 5.12
(a) Image corrupted by additive uniform noise. (b) Image additionally corrupted by additive salt-and-pepper noise. (c)-(f) Image (b) filtered with a 5×5: (c) arithmetic mean filter; (d) geometric mean filter; (e) median filter; (f) alpha-trimmed mean filter, with $d = 6$.

5.3 Restoration in the Presence of Noise Only—Spatial Filtering

5.3.3 Adaptive Filters

- Adaptive, local noise reduction filter

$$\hat{f}(x,y) = g(x,y) - \frac{\sigma_\eta^2}{\sigma_L^2}[g(x,y) - \bar{z}_{Sxy}] \qquad (5\text{-}32)$$

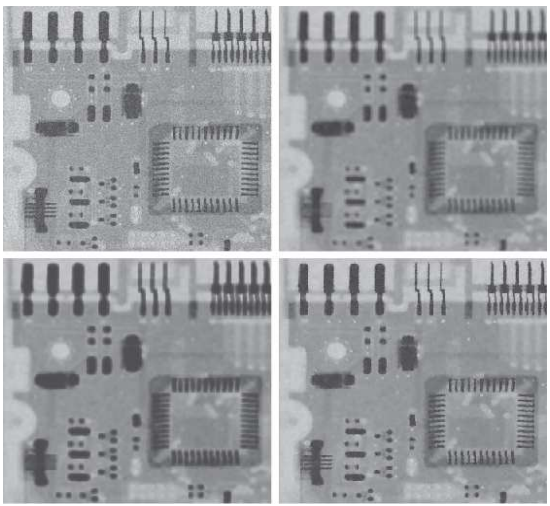

a b
c d

FIGURE 5.13
(a) Image corrupted by additive Gaussian noise of zero mean and a variance of 1000. (b) Result of arithmetic mean filtering. (c) Result of geometric mean filtering. (d) Result of adaptive noise-reduction filtering. All filters used were of size 7×7.

5.3 Restoration in the Presence of Noise Only—Spatial Filtering

5.3.3 Adaptive Filters

- Adaptive Median Filter

Stage A: $A1 = z_{med} - z_{min}$

$A2 = z_{med} - z_{max}$

If $A1 > 0$ AND $A2 < 0$, go to stage B

Else increase the window size

If window size $\leq S_{max}$ repeat stage A

Else output z_{xy}

Stage B: $B1 = z_{xy} - z_{min}$

$B2 = z_{xy} - z_{max}$

If $B1 > 0$ AND $B2 < 0$, output z_{xy}

Else output z_{med}

5.3 Restoration in the Presence of Noise Only—Spatial Filtering

5.3.3 Adaptive Filters

- Adaptive Median Filter

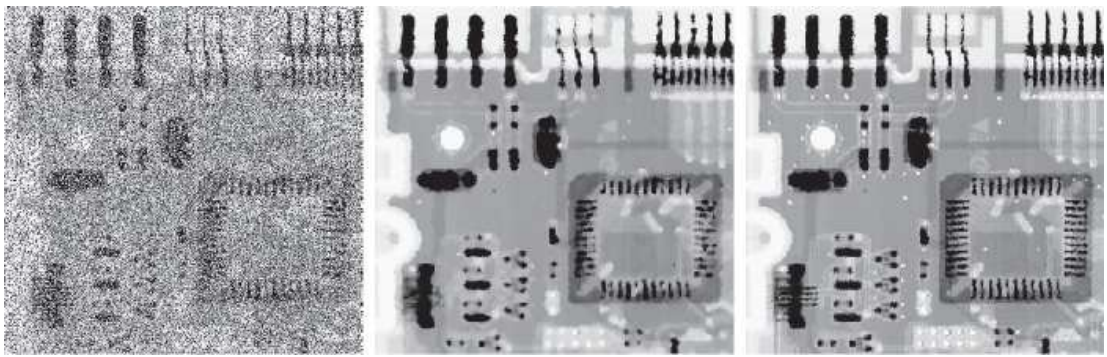

a b c

FIGURE 5.14 (a) Image corrupted by salt-and-pepper noise with probabilities $P_a = P_b = 0.25$. (b) Result of filtering with a 7×7 median filter. (c) Result of adaptive median filtering with $S_{max} = 7$.

5.4 Periodic Noise Reduction by Frequency Domain Filtering

5.4.1 More on Notch Filtering

$$H_{NP}(u,v) = 1 - H_{NR}(u,v) \qquad (5\text{-}37)$$

- Ideal Notch Reject Filter

$$H(u,v) = \begin{cases} 0 & \text{if } D_1(u,v) \le D_0 \text{ or } D_2(u,v) \le D_0 \\ 1 & \text{otherwise} \end{cases}$$

where $D_1(u,v) = [(u - M/2 - u_0)^2 + (v - N/2 - v_0)^2]^{1/2}$

$D_2(u,v) = [(u - M/2 + u_0)^2 + (v - N/2 + v_0)^2]^{1/2}$

- Butterworth Notch Reject Filter

$$H(u,v) = \frac{1}{1 + \left[\dfrac{D_0^2}{D_1(u,v)D_2(u,v)}\right]^n}$$

- Gaussian Notch Reject Filter

$$H(u,v) = 1 - e^{-\frac{1}{2}\left[\frac{D_1(u,v)D_2(u,v)}{D_0^2}\right]}$$

5.4 Periodic Noise Reduction by Frequency Domain Filtering

5.4.1 More on Notch Filtering

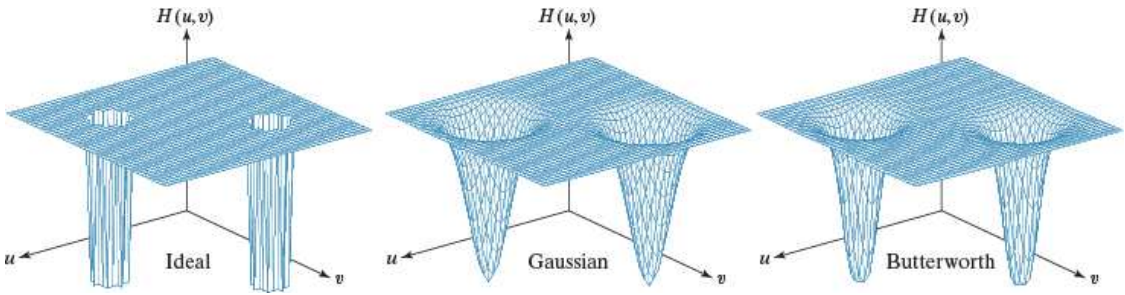

a b c

FIGURE 5.15 Perspective plots of (a) ideal, (b) Gaussian, and (c) Butterworth notch reject filter transfer functions.

5.4 Periodic Noise Reduction by Frequency Domain Filtering

5.4.1 More on Notch Filtering

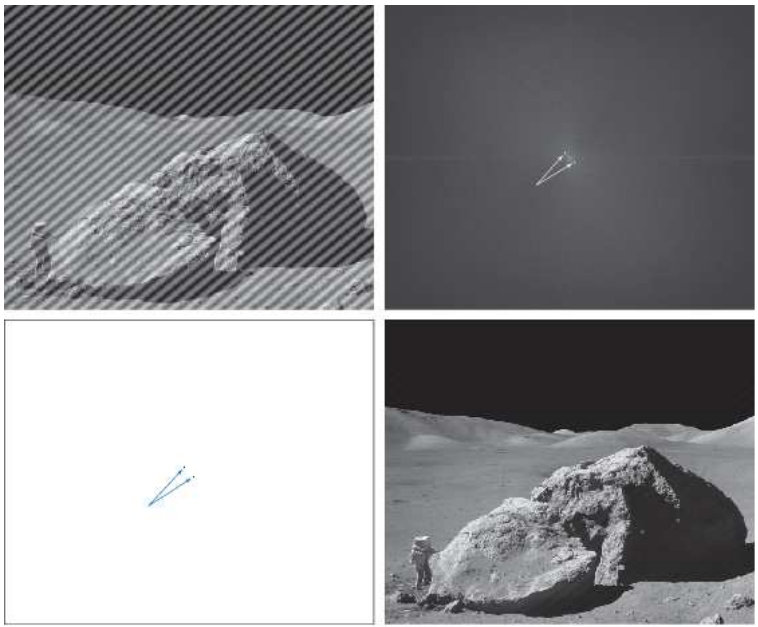

a b
c d

FIGURE 5.16
(a) Image corrupted by sinusoidal interference. (b) Spectrum showing the bursts of energy caused by the interference. (The bursts were enlarged for display purposes.) (c) Notch filter (the radius of the circles is 2 pixels) used to eliminate the energy bursts. (The thin borders are not part of the data.) (d) Result of notch reject filtering. (Original image courtesy of NASA.)

5.4 Periodic Noise Reduction by Frequency Domain Filtering

5.4.1 More on Notch Filtering

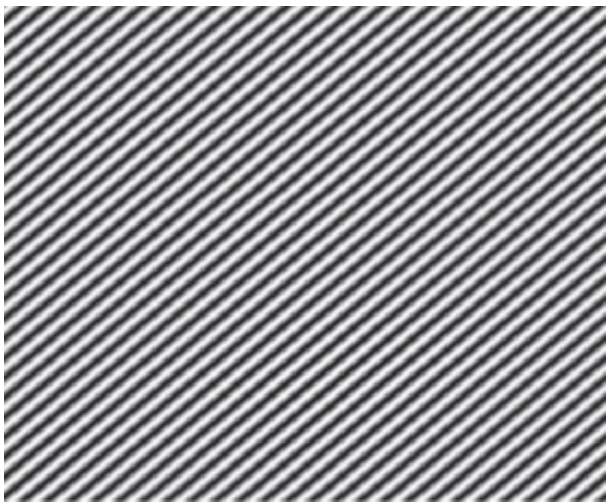

FIGURE 5.17 Sinusoidal pattern extracted from the DFT of Fig. 5.16(a) using a notch pass filter.

5.4 Periodic Noise Reduction by Frequency Domain Filtering

5.4.1 More on Notch Filtering

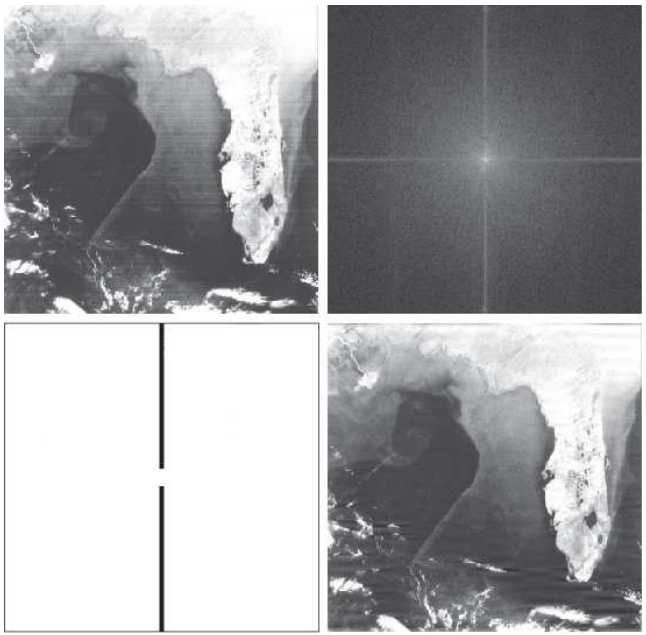

a b
c d

FIGURE 5.18
(a) Satellite image of Florida and the Gulf of Mexico. (Note horizontal sensor scan lines.) (b) Spectrum of (a). (c) Notch reject filter transfer function. (The thin black border is not part of the data.) (d) Filtered image. (Original image courtesy of NOAA.)

5.4 Periodic Noise Reduction by Frequency Domain Filtering

5.4.1 More on Notch Filtering

FIGURE 5.19
Noise pattern extracted from Fig. 5.18(a) by notch pass filtering.

5.4 Periodic Noise Reduction by Frequency Domain Filtering

5.4.2 Optimum Notch Filtering

a b

FIGURE 5.20
(a) Image of the Martian terrain taken by Mariner 6. (b) Fourier spectrum showing periodic interference. (Courtesy of NASA.)

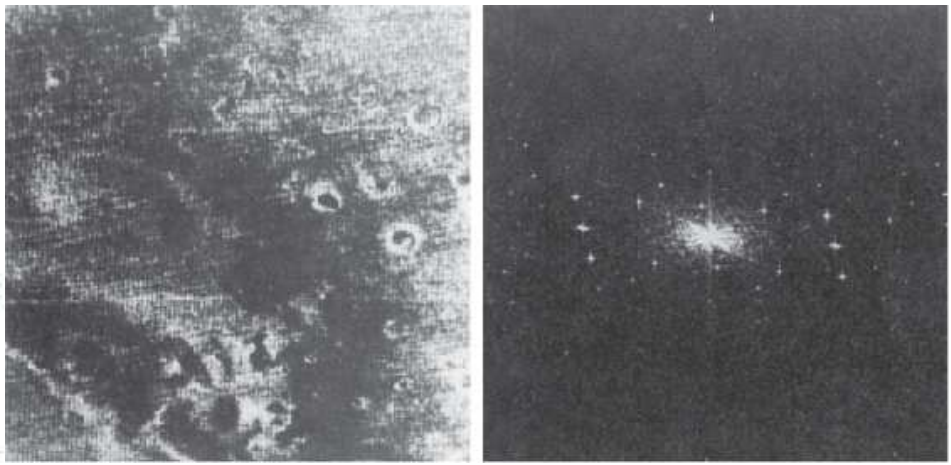

5.4 Periodic Noise Reduction by Frequency Domain Filtering

5.4.2 Optimum Notch Filtering

$$N(u,v) = H(u,v)\,G(u,v) \tag{5-38}$$

$$\eta(x,y) = \Im^{-1}\{H(u,v)\,G(u,v)\} \tag{5-39}$$

$$\hat{f}(x,y) = g(x,y) - w(x,y)\eta(x,y) \tag{5-40}$$

$\eta(x,y)$ is noise, $w(x,y)$ is a weighing or modulation function.

$$\sigma^2(x,y) = \frac{1}{mn}\sum_{(r,c)\in S_{xy}}\left[\hat{f}(r,c) - \bar{\hat{f}}\right] \tag{5-41}$$

$$\bar{\hat{f}}(x,y) = \frac{1}{mn}\sum_{(r,c)\in S_{xy}}\hat{f}(r,c) \tag{5-42}$$

$$\sigma^2(x,y) = \sum_{(r,c)\in S_{xy}}\left\{\left[g(r,c) - w(r,c)\eta(r,c)\right] - \left[\bar{g} - \overline{w\eta}\right]\right\}^2 \tag{5-43}$$

5.4 Periodic Noise Reduction by Frequency Domain Filtering

5.4.2 Optimum Notch Filtering

Assume

$$w(r,c) = w(x,y) \tag{5-44}$$

Then we have

$$\overline{w\eta} = w(x,y)\bar{\eta} \tag{5-45}$$

$$\sigma^2(x,y) = \sum_{(r,c)\in S_{xy}} \left\{\left[g(r,c) - w(x,y)\eta(r,c)\right] - \left[\bar{g} - w(x,y)\bar{\eta}\right]\right\}^2 \tag{5-46}$$

to get the minimum of $\sigma^2(x,y)$, we can solve the following equation:

$$\frac{\partial \sigma^2(x,y)}{\partial w(x,y)} = 0 \tag{5-47}$$

$$w(x,y) = \frac{\overline{g\eta} - \bar{g}\bar{\eta}}{\overline{\eta^2} - \bar{\eta}^2} \tag{5-48}$$

5.4 Periodic Noise Reduction by Frequency Domain Filtering

5.4.2 Optimum Notch Filtering

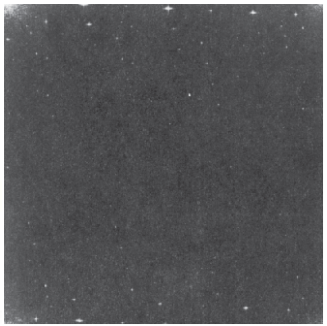

FIGURE 5.21 Uncentered Fourier spectrum of the image in Fig. 5.20(a). (Courtesy of NASA.)

a b

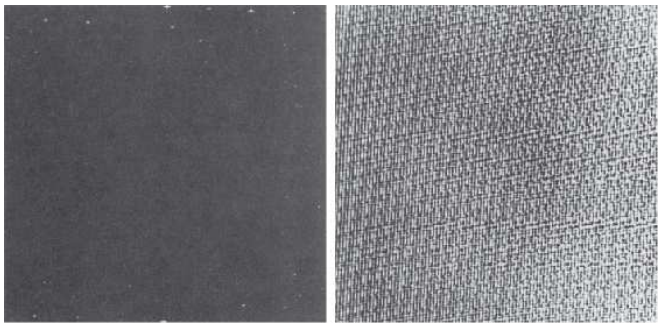

FIGURE 5.22 (a) Fourier spectrum of $N(u,v)$, and (b) corresponding spatial noise interference pattern, $\eta(x,y)$. (Courtesy of NASA.)

5.4 Periodic Noise Reduction by Frequency Domain Filtering

5.4.2 Optimum Notch Filtering

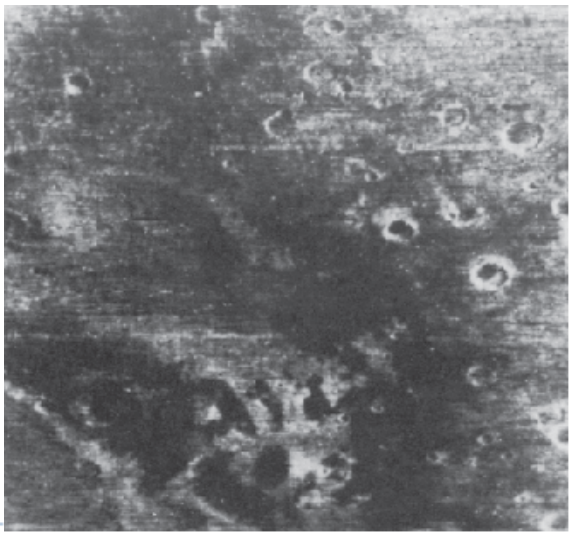

FIGURE 5.23 Restored image. (Courtesy of NASA.)

5.5 Linear, Position-Invariant Degradations

- Definition

1. input-output relationship

$$g(x,y) = H\,[f(x,y)] + \eta(x,y) \qquad (5\text{-}49)$$

2. Linearity

$$H[\,a\,f_1(x,y) + b\,f_2(x,y)\,] = a\,H[\,f_1(x,y)] + b\,H[\,f_2(x,y)\,] \qquad (5\text{-}50)$$

3. Additivity

$$H[f_1(x,y) + f_2(x,y)\,] = H[f_1(x,y)] + H[f_2(x,y)] \qquad (5\text{-}51)$$

4. Homogeneity

$$H[a\,f_1(x,y)] = a\,H[f_1(x,y)\,] \qquad (5\text{-}52)$$

5. Space Invariant

$$H\,f(\,x-\alpha,\,y-\beta\,) = g(x-\alpha,\,y-\beta\,) \qquad (5\text{-}53)$$

5.5 Linear, Position-Invariant Degradations

- Degradation of continuous function

Applying the concept of sampling or Impulse Function, $f(x, y)$ can be expressed in the following formula ：

$$f(x,y) = \int_{-\infty}^{\infty}\int_{-\infty}^{\infty} f(\alpha,\beta)\delta(x-\alpha, y-\beta)d\alpha d\beta \qquad (5\text{-}54)$$

If $\eta(x,y) = 0$, then the definition of degradations is available:

$$g(x,y) = Hf(x,y) = H\int_{-\infty}^{\infty}\int_{-\infty}^{\infty} f(\alpha,\beta)\delta(x-\alpha, y-\beta)d\alpha d\beta \qquad (5\text{-}55)$$

Assuming H is a linear operator and the additive of the integral is true, then:

$$g(x,y) = \int_{-\infty}^{\infty}\int_{-\infty}^{\infty} H[f(\alpha,\beta)\delta(x-\alpha, y-\beta)]d\alpha d\beta \qquad (5\text{-}56)$$

Since $f(\alpha, \beta)$ is independent of x, y, and using the homogeneity properties, it follows that:

$$g(x,y) = \int_{-\infty}^{\infty}\int_{-\infty}^{\infty} f(\alpha,\beta)H[\delta(x-\alpha, y-\beta)]d\alpha d\beta \qquad (5\text{-}57)$$

5.5 Linear, Position-Invariant Degradations

- Degradation of continuous function

$$h(x,\alpha,y,\beta) = H[\delta(x-\alpha, y-\beta)] \qquad (5\text{-}58)$$

$h(x, \alpha, y, \beta)$ is called the Impulse Response of H, and $h(x, \alpha, y, \beta)$ in optics is commonly referred to as Point Spread Function (PSF). Substituting (5.5-10) into (5.5-9)

$$g(x,y) = \int_{-\infty}^{\infty}\int_{-\infty}^{\infty} f(\alpha,\beta)h(x,\alpha,y,\beta)d\alpha d\beta \qquad (5\text{-}59)$$

If H is position invariant, then

$$H[\delta(x,\alpha,y,\beta)] = h(x-\alpha, y-\beta) \qquad (5\text{-}60)$$

Therefore (5-59) reduces to

$$g(x,y) = \int_{-\infty}^{\infty}\int_{-\infty}^{\infty} f(\alpha,\beta)h(x-\alpha,y-\beta)d\alpha d\beta \qquad (5\text{-}61)$$

5.5 Linear, Position-Invariant Degradations

- Degradation of continuous function

From equation (5-61), if the impulse response of a linear system is known, the output $g(x, y)$ of the linear system can be calculated from the input $f(x, y)$. If the noise is present, then (5-59) becomes:

$$g(x,y) = \int_{-\infty}^{\infty}\int_{-\infty}^{\infty} f(\alpha,\beta)h(x,\alpha,y,\beta)d\alpha d\beta + \eta(x,y) \qquad (5\text{-}62)$$

If H is position invariant, then

$$g(x,y) = \int_{-\infty}^{\infty}\int_{-\infty}^{\infty} f(\alpha,\beta)h(x-\alpha,y-\beta)d\alpha d\beta + \eta(x,y) \qquad (5\text{-}63)$$

Using the familiar notation for convolution, the above formula is:

$$g(x,y) = h(x,y) \star f(x,y) + \eta(x,y) \qquad (5\text{-}64)$$

$$G(u,v) = H(u,v)F(u,v) + N(u,v) \qquad (5\text{-}65)$$

5.6 Estimating the Degradation Function

5.6.1 Estimation by Image Observation

1. Take a sub-image $g_s(x, y)$ with a strong signal in the image
2. Create ideal image $f(x, y)$ of the same size as $g_s(x, y)$
3. Assuming that the noise impact is small, according to (5-65),we can use the following formula to estimate the degradation function

$$H_s(u,v) = \frac{G_s(u,v)}{\hat{F}_s(u,v)} \qquad (5\text{-}66)$$

5.6 Estimating the Degradation Function

5.6.2 Estimation by Experimentation

1. Adjust the camera and set parameters to get an image similar to degraded image
2. Obtain the impulse response by small dot of light using the same system setting
3. Calculate the degradation function according to the impulse response obtained by the following formula

$$H_s(u,v) = \frac{G_s(u,v)}{A} \qquad (5\text{-}67)$$

a b

FIGURE 5.24 Estimating a degradation by impulse characterization. (a) An impulse of light (shown magnified). (b) Imaged (degraded) impulse.

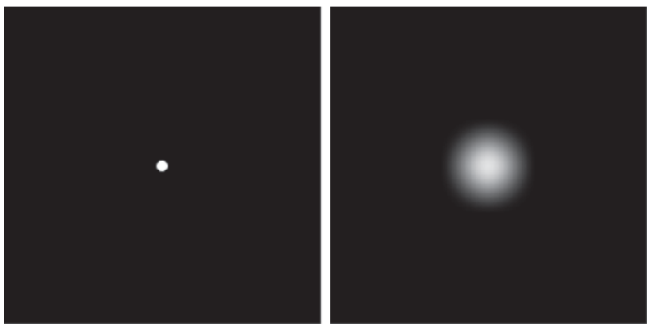

5.6 Estimating the Degradation Function

5.6.3 Estimation by Modeling

- Image degradation by atmospheric turbulence

$$H(u,v) = e^{-k(u^2+v^2)^{5/6}} \qquad (5\text{-}68)$$

a b
c d

FIGURE 5.25 Modeling turbulence. (a) No visible turbulence. (b) Severe turbulence, $k = 0.0025$. (c) Mild turbulence, $k = 0.001$. (d) Low turbulence, $k = 0.00025$. All images are of size 480×480 pixels. (Original image courtesy of NASA.)

5.6 Estimating the Degradation Function

5.6.3 Estimation by Modeling

- Uniform linear motion image degradation model

$$g(x,y) = \int_0^T f[x - x_0(t), y - y_0(t)]dt \qquad (5\text{ - }69)$$

$$G(u,v) = \int_{-\infty}^{\infty}\int_{-\infty}^{\infty} g(x,y)e^{-j2\pi(ux+vy)}dxdy$$

$$= \int_{-\infty}^{\infty}\int_{-\infty}^{\infty}\left[\int_0^T f[x - x_0(t), y - y_0(t)]dt\right]e^{-j2\pi(ux+vy)}dxdy \qquad (5\text{ - }71)$$

$$G(u,v) = \int_0^T\left[\int_{-\infty}^{\infty}\int_{-\infty}^{\infty} f[x - x_0(t), y - y_0(t)]e^{-j2\pi(ux+vy)}dxdy\right]dt \qquad (5\text{ - }72)$$

$$G(u,v) = \int_0^T F(u,v)e^{-j2\pi[ux_0(t)+vy_0(t)]}dt$$

$$= F(u,v)\int_0^T e^{-j2\pi[ux_0(t)+vy_0(t)]}dt \qquad (5\text{ - }73)$$

$$\text{let} \quad H(u,v) = \int_0^T e^{-j2\pi[ux_0(t)+vy_0(t)]}dt \qquad (5\text{ - }74)$$

$$\text{then} \quad G(u,v) = H(u,v)F(u,v) \qquad (5\text{ - }75)$$

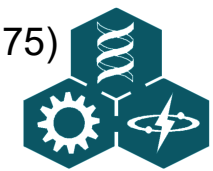

5.6 Estimating the Degradation Function

5.6.3 Estimation by Modeling

- Uniform linear motion image degradation model

$$H(u,v) = \int_0^T e^{-j2\pi u x_0(t)} dt = \int_0^T e^{-j2\pi u a t/T} dt = \frac{T}{\pi u a} \sin(\pi u a) e^{-j\pi u a} \quad (5\text{ - }76)$$

$$H(u,v) = \frac{T}{\pi(ua+vb)} \sin[\,\pi(ua+vb)\,] e^{-j\pi(ua+vb)} \quad (5\text{ - }77)$$

a b

FIGURE 5.26
(a) Original image. (b) Result of blurring using the function in Eq. (5-77) with $a = b = 0.1$ and $T = 1$.

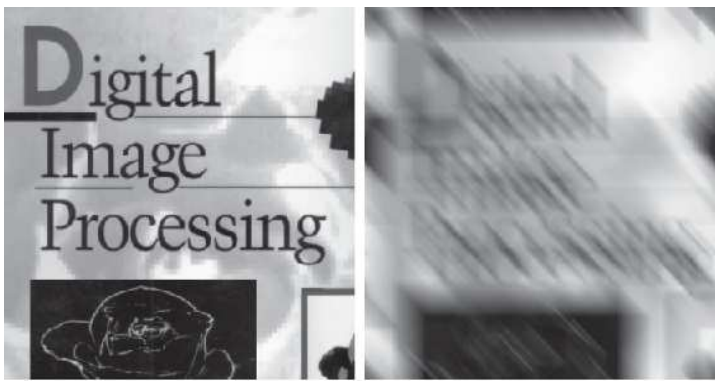

5.7 Inverse Filtering

$$\hat{F}(u,v) = \frac{G(u,v)}{H(u,v)} \qquad (5\text{-}78)$$

$$\hat{F}(u,v) = F(u,v) + \frac{N(u,v)}{H(u,v)} \qquad (5\text{-}79)$$

- Problem of restoration with (5-79)
  - The noise $N(u,v)$ is a random function
  - The case where the value of $H(u,v)$ is zero or a small value

5.7 Inverse Filtering

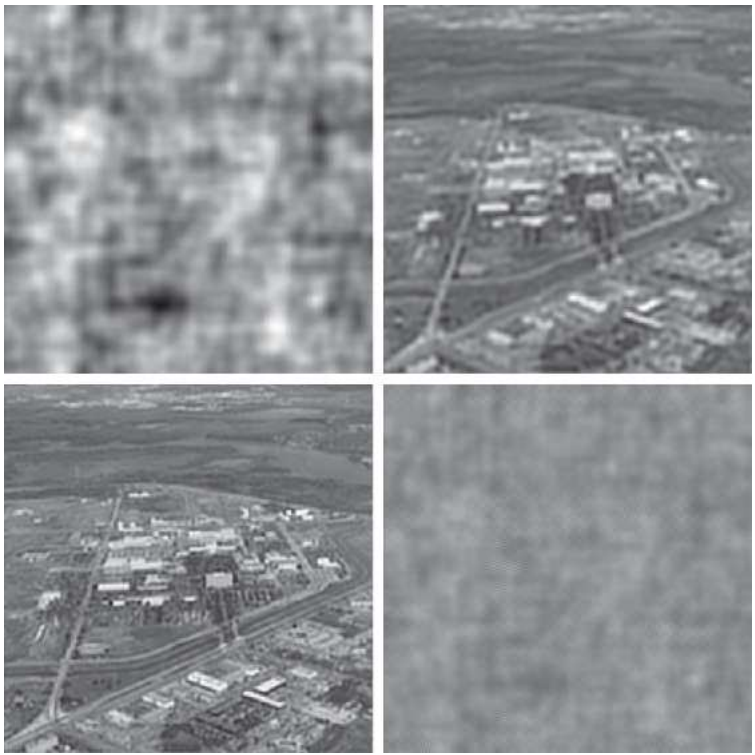

a b
c d

FIGURE 5.27 Restoring Fig. 5.25(b) using Eq. (5-78). (a) Result of using the full filter. (b) Result with H cut off outside a radius of 40. (c) Result with H cut off outside a radius of 70. (d) Result with H cut off outside a radius of 85.

5.8 Minimum Mean Square Error (Wiener) Filtering

- Wiener Filter

$$e^2 = E\{(f - \hat{f})^2\} \tag{5-80}$$

$$\hat{F}(u,v) = \left[\frac{H^*(u,v)S_f(u,v)}{S_f(u,v)|H(u,v)|^2 + S_\eta(u,v)}\right]G(u,v)$$

$$= \left[\frac{H^*(u,v)}{|H(u,v)|^2 + S_\eta(u,v)/S_f(u,v)}\right]G(u,v)$$

$$= \left[\frac{1}{H(u,v)}\frac{|H(u,v)|^2}{|H(u,v)|^2 + S_\eta(u,v)/S_f(u,v)}\right]G(u,v) \tag{5-81}$$

When it is white noise in the degradation image

$$\hat{F}(u,v) = \left[\frac{1}{H(u,v)}\frac{|H(u,v)|^2}{|H(u,v)|^2 + K}\right]G(u,v) \tag{5-85}$$

5.8 Minimum Mean Square Error (Wiener) Filtering

- Wiener Filter

a b c

FIGURE 5.28 Comparison of inverse and Wiener filtering. (a) Result of full inverse filtering of Fig. 5.25(b). (b) Radially limited inverse filter result. (c) Wiener filter result.

5.8 Minimum Mean Square Error (Wiener) Filtering

- Wiener Filter

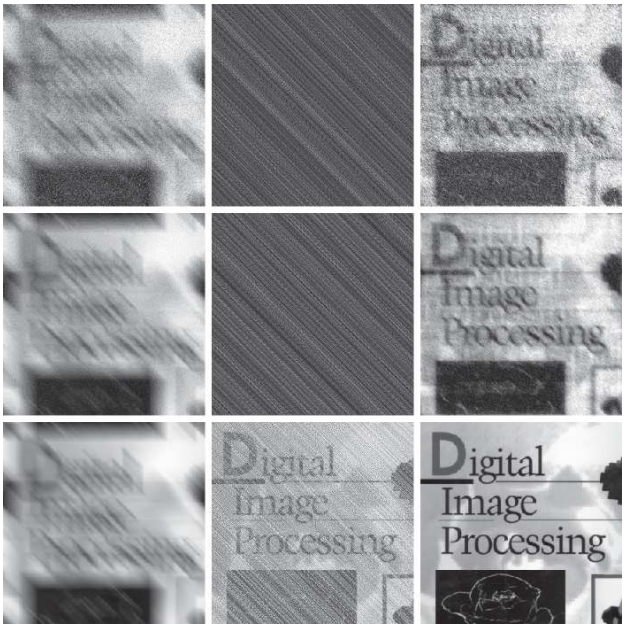

FIGURE 5.29 (a) 8-bit image corrupted by motion blur and additive noise. (b) Result of inverse filtering. (c) Result of Wiener filtering. (d)–(f) Same sequence, but with noise variance one order of magnitude less. (g)–(i) Same sequence, but noise variance reduced by five orders of magnitude from (a). Note in (h) how the deblurred image is quite visible through a "curtain" of noise.

5.8 Minimum Mean Square Error (Wiener) Filtering

- Wiener Filter

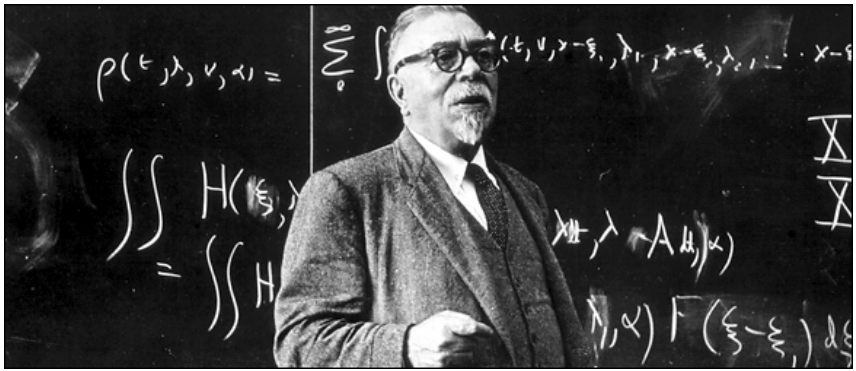

Image courtesy of the Research Laboratory of Electronics at MIT.

Norbert Wiener (November 26, 1894 - March 18, 1964) was an American mathematician, known as the founder of cybernetics. He created the term in his book Cybernetics or Control and Communication in the Animal and the Machine (MIT Press, 1948), widely recognized as one of the most important books of contemporary scientific thinking. Additionally, he is thought to be the first American-born and American-trained mathematician able to spar intellectually with anything or anyone Europe and the historic bastions of mathematics could proffer. His period thus represents a watershed in American mathematics.

5.9 Constrained Least Squares Filtering

Express degradation in vector-matrix form

$$\mathbf{g} = \mathbf{H}\,\mathbf{f} + \boldsymbol{\eta} \qquad (5\text{-}86)$$

Find the minimum of the following formula

$$C = \sum_{x=0}^{M-1}\sum_{y=0}^{N-1}\left[\nabla^2 f(x,y)\right]^2 \qquad (5\text{-}87)$$

The restrictions are:

$$\left\|\mathbf{g} - \mathbf{H}\,\hat{\mathbf{f}}\right\|^2 = \|\boldsymbol{\eta}\|^2 \qquad (5\text{-}88)$$

The solution to this optimization problem is

$$\hat{F}(u,v) = \left[\frac{H^*(u,v)}{|H(u,v)|^2 + \gamma|P(u,v)|^2}\right] G(u,v) \qquad (5\text{-}89)$$

γ is a parameter that adjusts to meet the constraint condition, and $P(u, v)$ is a Fourier transform of the following formula

$$p(x,y) = \begin{bmatrix} 0 & -1 & 0 \\ -1 & 4 & -1 \\ 0 & -1 & 0 \end{bmatrix} \qquad (5\text{-}90)$$

5.9 Constrained Least Squares Filtering

a b c

FIGURE 5.30 Results of constrained least squares filtering. Compare (a), (b), and (c) with the Wiener filtering results in Figs. 5.29(c), (f), and (i), respectively.

5.9 Constrained Least Squares Filtering

- Iterative method to find parameter γ

define $\mathbf{r} = \mathbf{g} - \mathbf{H}\hat{\mathbf{f}}$ (5-91)

$$\varphi(\gamma) = \mathbf{r}^T\mathbf{r} = \|\mathbf{r}\|^2 \quad (5\text{-}92)$$

$\varphi(\gamma)$ is a monotonically increasing function, so you can use iterative method to adjust γ to meet

$$\|\mathbf{r}\|^2 = \|\boldsymbol{\eta}\|^2 \pm a \quad (5\text{-}93)$$

$\|\mathbf{r}\|^2$ and $\|\boldsymbol{\eta}\|^2$ can be calculated as follows:

$$R(u,v) = G(u,v) - H(u,v)\hat{F}(u,v) \quad (5\text{-}94)$$

$$\|\mathbf{r}\|^2 = \sum_{x=0}^{M-1}\sum_{y=0}^{N-1} r^2(x,y) \quad (5\text{-}95)$$

$$\sigma_\eta^2 = \sum_{x=0}^{M-1}\sum_{y=0}^{N-1}\left[\eta(x,y) - m_\eta\right]^2 \quad (5\text{-}96)$$

$$m_\eta = \sum_{x=0}^{M-1}\sum_{y=0}^{N-1}\eta(x,y) \quad (5\text{-}97)$$

$$\|\boldsymbol{\eta}\|^2 = MN\left[\sigma_\eta^2 - m_\eta\right] \quad (5\text{-}98)$$

5.9 Constrained Least Squares Filtering

a b

FIGURE 5.31
(a) Iteratively determined constrained least squares restoration of Fig. 5.25(b), using correct noise parameters. (b) Result obtained with wrong noise parameters.

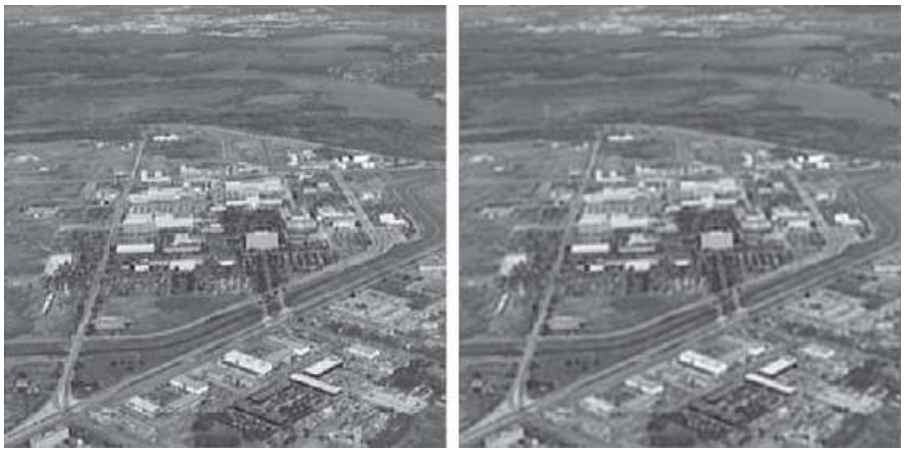

5.10 Geometric Mean Filter

- Generalization of Wiener filters

$$\hat{F}(u,v)=\left[\frac{H^*(u,v)}{|H(u,v)|^2}\right]^{\alpha}\left[\frac{H^*(u,v)}{|H(u,v)|^2+\beta\left[\frac{S_\eta(u,v)}{S_f(u,v)}\right]}\right]^{1-\alpha}G(u,v) \qquad (5\text{-}99)$$

$\alpha=1$, Inverse Filter
$\alpha=0$, Parametric Wiener Filter
$\alpha=0$, $\beta=1$, Standard Wiener Filter
$\alpha=1/2$, $\beta=1$, Spectrum Equalization Filter

5.10 Geometric Mean Filter

- Deep Learning Approach

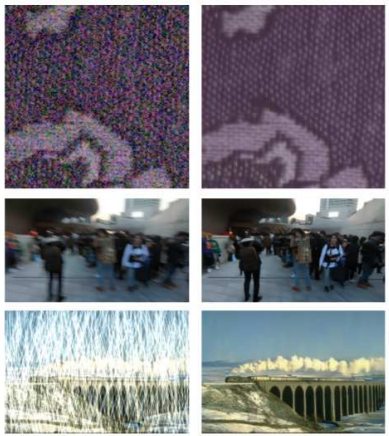

Figure 1: Visualized results of HINet on various image restoration tasks. Left: degraded image. Right: the predicted result of HINet. From top to bottom: image denoising, image deblurring, and image deraining task respectively.

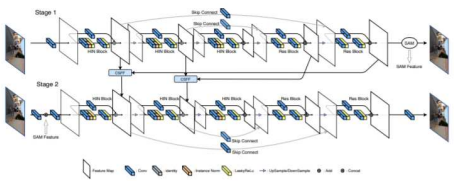

Figure 2: Proposed Half Instance Normalization Network (HINet). The encoder of each subnetwork contains Half Instance Normalization Blocks (HIN Block). For simplicity, we only show 3 layers of HIN Block in the figure, and HINet has a total of 5 layers. We adopt CSFF and SAM modules from MPRNet [56].

Source: https://paperswithcode.com/task/deblurring

5.10 Geometric Mean Filter

- Deep Learning Approach

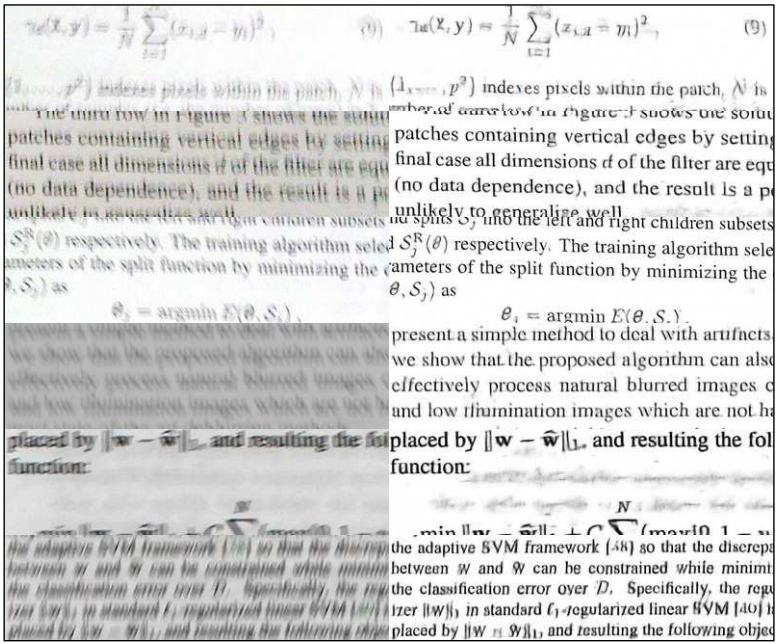

$$\gamma_{\mathrm{R}}(\mathbf{x}, \mathbf{y}) = \frac{1}{N} \sum_{i=1}^{N} (x_{i,R} - y_i)^2, \quad (9)$$

$(1, \ldots, p^2)$ indexes pixels within the patch, N is

patches containing vertical edges by setting

final case all dimensions d of the filter are equ

(no data dependence), and the result is a p

unlikely to generalize well.

$\mathcal{S}_j^{\mathrm{R}}(\theta)$ respectively. The training algorithm sele

ameters of the split function by minimizing the

$\theta, \mathcal{S}_j)$ as

$$\theta_j = \operatorname{argmin}_{\theta} E(\theta, \mathcal{S}_j).$$

present a simple method to deal with artifacts

we show that the proposed algorithm can als

effectively process natural blurred images

and low illumination images which are not ha

placed by $\|\mathbf{w} - \hat{\mathbf{w}}\|_1$ and resulting the fol

function:

$$\min_{\mathbf{w}, \hat{\mathbf{w}}} \|\mathbf{w} - \hat{\mathbf{w}}\|_1 + C \sum_{n=1}^{N} (\max[0, 1 - y_n$$

the adaptive SVM framework [48] so that the discrepa

between w and $\hat{w}$ can be constrained while minimi

the classification error over $\mathcal{D}$. Specifically, the regu

izer $\|w\|_1$ in standard ℓ_1-regularized linear SVM [40] i

placed by $\|w - \hat{w}\|_1$, and resulting the following objec

Source: Convolutional Neural Networks for Direct Text Deblurring (Hradiš et al., 2015)

5.11 Image Reconstruction from Projections

5.11.1 Introduction

- Backprojection

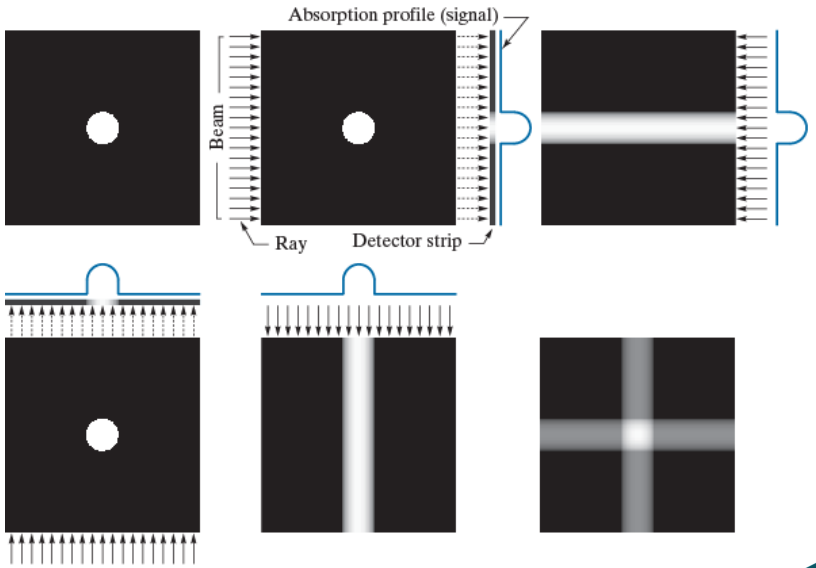

a b c
d e f

FIGURE 5.32
(a) Flat region with a single object. (b) Parallel beam, detector strip, and profile of sensed 1-D absorption signal. (c) Result of back-projecting the absorption profile. (d) Beam and detectors rotated by 90°. (e) Backprojection. (f) The sum of (c) and (e), intensity-scaled. The intensity where the backprojections intersect is twice the intensity of the individual back-projections.

5.11 Image Reconstruction from Projections

5.11.1 Introduction

- Image reconstruction with backprojection

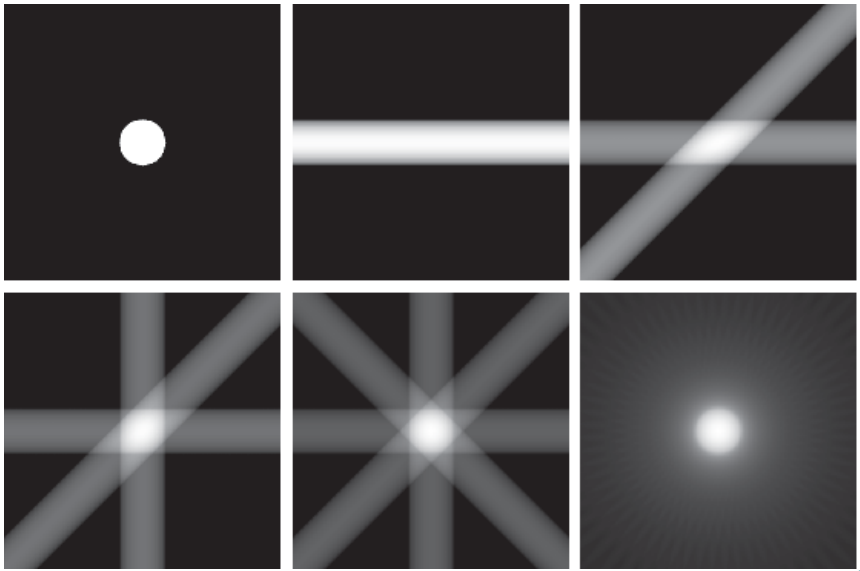

a b c
d e f

FIGURE 5.33
(a) Same as Fig. 5.32(a). (b)-(e) Reconstruction using 1, 2, 3, and 4 backprojections 45° apart. (f) Reconstruction with 32 backprojections 5.625° apart (note the blurring).

5.11 Image Reconstruction from Projections

5.11.1 Introduction

- Image reconstruction with backprojection

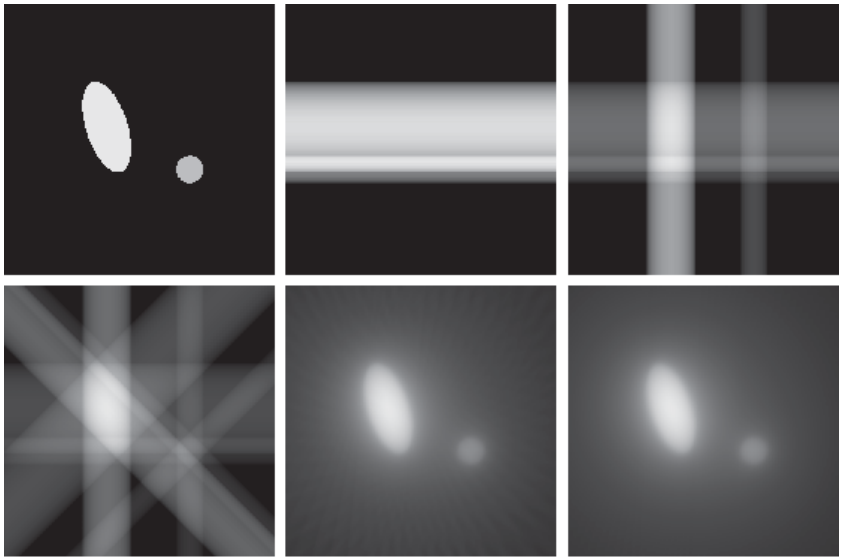

a b c
d e f

FIGURE 5.34
(a) Two objects with different absorption characteristics. (b)–(d) Reconstruction using 1, 2, and 4 backprojections, 45° apart. (e) Reconstruction with 32 backprojections, 5.625° apart. (f) Reconstruction with 64 backprojections, 2.8125° apart.

5.11 Image Reconstruction from Projections

5.11.2 Principles of Computed Tomography (CT)

- Nobel Prize in Medicine, 1979, Cormack and Hounsfield

Godfrey N. Hounsfield

Allan M. Cormack

Source: http://nobelprize.org/

5.11 Image Reconstruction from Projections

5.11.2 Principles of Computed Tomography (CT)

- Four generations of CT scanners

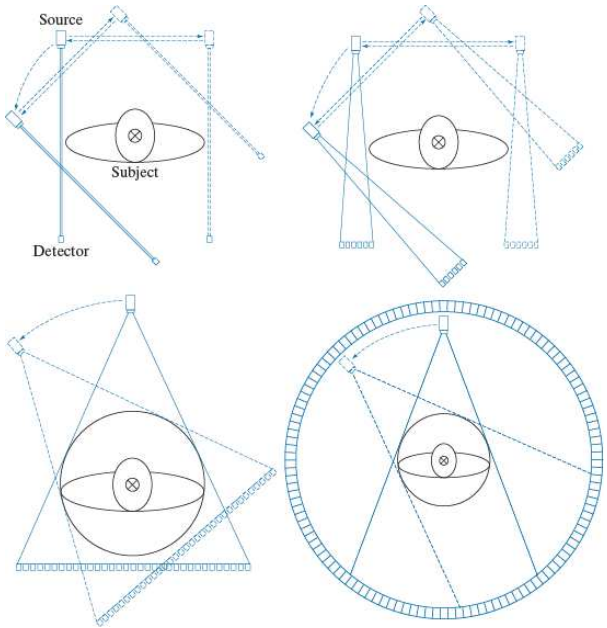

a b
c d

FIGURE 5.35
Four generations of CT scanners. The dotted arrow lines indicate incremental linear motion. The dotted arrow arcs indicate incremental rotation. The cross-mark on the subject's head indicates linear motion perpendicular to the plane of the paper. The double arrows in (a) and (b) indicate that the source/detector unit is translated and then brought back into its original position.

5.11 Image Reconstruction from Projections

5.11.3 Projections and the Radon Transform

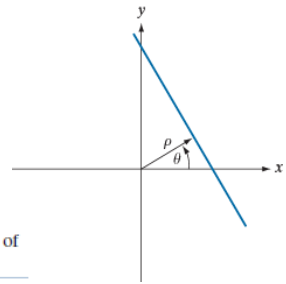

FIGURE 5.36
Normal representation of a line.

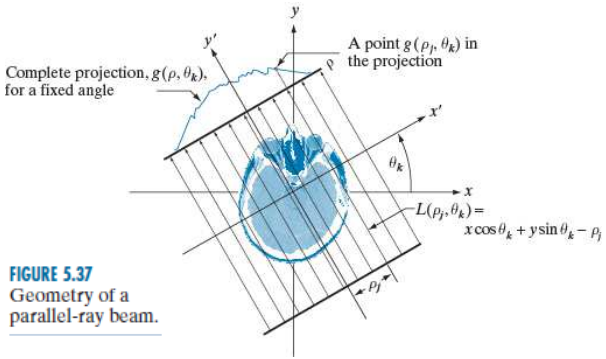

FIGURE 5.37
Geometry of a parallel-ray beam.

$$x\cos\theta + y\sin\theta = \rho \qquad (5\text{-}100)$$

$$g(\rho_j, \theta_k) = \int_{-\infty}^{\infty}\int_{-\infty}^{\infty} f(x,y)\delta(x\cos\theta_k + y\sin\theta_k - \rho_j)dxdy \qquad (5\text{-}101)$$

$$g(\rho,\theta) = \int_{-\infty}^{\infty}\int_{-\infty}^{\infty} f(x,y)\delta(x\cos\theta + y\sin\theta - \rho)dxdy \qquad (5\text{-}102)$$

$$g(\rho,\theta) = \sum_{x=0}^{M-1}\sum_{y=0}^{N-1} f(x,y)\delta(x\cos\theta + y\sin\theta - \rho) \qquad (5\text{-}103)$$

5.11 Image Reconstruction from Projections

5.11.3 Projections and the Radon Transform

- Example

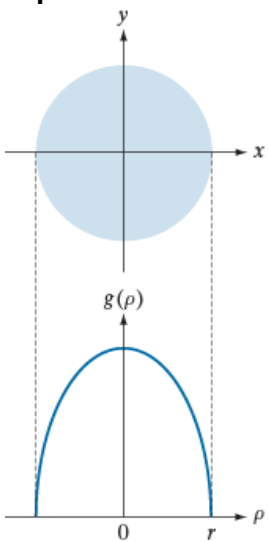

a
b

FIGURE 5.38
(a) A disk and, (b) a plot of its Radon transform, derived analytically. Here we were able to plot the transform because it depends only on one variable. When g depends on both ρ and θ, the Radon transform becomes an image whose axes are ρ and θ, and the intensity of a pixel is proportional to the value of g at the location of that pixel.

$$f(x,y)=\begin{cases}A & x^2+y^2\le r^2\\ 0 & \text{otherwise}\end{cases}$$

$$g(\rho,\theta)=\int_{-\infty}^{\infty}\int_{-\infty}^{\infty}f(x,y)\delta(x-\rho)dxdy$$

$$=\int_{-\infty}^{\infty}f(\rho,y)dy$$

$$g(\rho,\theta)=\int_{-\sqrt{r^2-\rho^2}}^{\sqrt{r^2-\rho^2}}f(\rho,y)dy$$

$$=\int_{-\sqrt{r^2-\rho^2}}^{\sqrt{r^2-\rho^2}}Ady$$

$$g(\rho,\theta)=g(\rho)=\begin{cases}2A\sqrt{r^2-\rho^2} & |\rho|\le r\\ 0 & \text{otherwise}\end{cases}$$

5.11 Image Reconstruction from Projections

5.11.3 Projections and the Radon Transform

- Sinogram

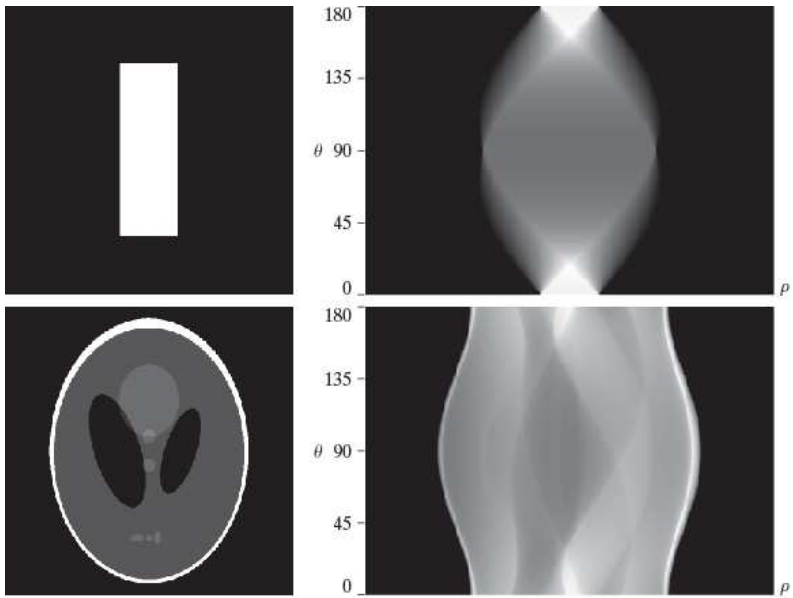

a b
c d

FIGURE 5.39
Two images and their sinograms (Radon transforms). Each row of a sinogram is a projection along the corresponding angle on the vertical axis. (Note that the horizontal axis of the sinograms are values of ρ.) Image (c) is called the *Shepp-Logan phantom*. In its original form, the contrast of the phantom is quite low. It is shown enhanced here to facilitate viewing.

5.11 Image Reconstruction from Projections

5.11.3 Projections and the Radon Transform

- Backprojection reconstruction image by Radon Transform

$$f_{\theta_k}(x,y) = g(\rho,\theta_k) = g(x\cos\theta_k + y\sin\theta_k, \theta_k)$$

$$f_\theta(x,y) = g(x\cos\theta + y\sin\theta, \theta) \qquad (5\text{-}104)$$

$$f(x,y) = \int_0^\pi f_\theta(x,y)\,d\theta \qquad (5\text{-}105)$$

$$f(x,y) = \sum_{\theta=0}^{\pi} f_\theta(x,y) \qquad (5\text{-}106)$$

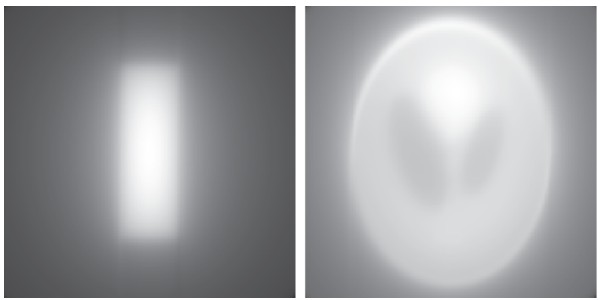

a b

FIGURE 5.40 Backprojections of the sinograms in Fig. 5.39.

5.11 Image Reconstruction from Projections

5.11.4 The Fourier-Slice Theorem

1-D Fourier transform for one projection θ

$$G(\omega,\theta)=\int_{-\infty}^{\infty} g(\rho,\theta)e^{-j2\pi\omega\rho}d\rho \qquad (5\text{-}107)$$

$$\begin{aligned} G(\omega,\theta) &= \int_{-\infty}^{\infty}\int_{-\infty}^{\infty}\int_{-\infty}^{\infty} f(x,y)\delta(x\cos\theta+y\sin\theta-\rho)e^{-j2\pi\omega\rho}dxdyd\rho \\ &= \int_{-\infty}^{\infty}\int_{-\infty}^{\infty} f(x,y)\left[\int_{-\infty}^{\infty}\delta(x\cos\theta+y\sin\theta-\rho)e^{-j2\pi\omega\rho}d\rho\right]dxdy \\ &= \int_{-\infty}^{\infty}\int_{-\infty}^{\infty} f(x,y)e^{-j2\pi\omega(x\cos\theta+y\sin\theta)}dxdy \qquad (5\text{-}108) \end{aligned}$$

$$G(\omega,\theta)=\left[\int_{-\infty}^{\infty}\int_{-\infty}^{\infty} f(x,y)e^{-j2\pi\omega(ux+vy)}dxdy\right]_{u=\omega\cos\theta;v=\omega\sin\theta} \qquad (5\text{-}109)$$

$$\begin{aligned} G(\omega,\theta) &= \left[F(u,v)\right]_{u=\omega\cos\theta;v=\omega\sin\theta} \\ &= F(\omega\cos\theta,\omega\sin\theta) \qquad (5\text{-}110) \end{aligned}$$

5.11 Image Reconstruction from Projections

5.11.4 The Fourier-Slice Theorem

- The Fourier transform of a projection is a slice of the 2-D Fourier transform of the region from which the projection was obtained.

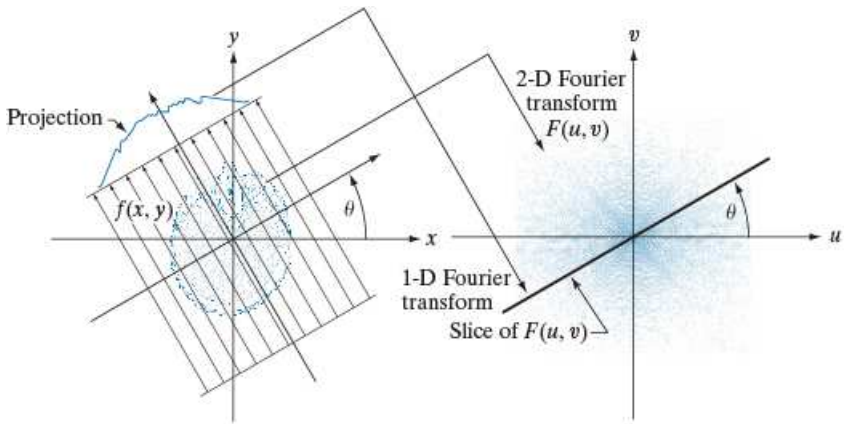

FIGURE 5.41 Illustration of the Fourier-slice theorem. The 1-D Fourier transform of a projection is a slice of the 2-D Fourier transform of the region from which the projection was obtained. Note the correspondence of the angle θ in the two figures.

5.11 Image Reconstruction from Projections

5.11.5 Reconstruction Using Parallel-Beam Filtered Backprojections

- Filtered backprojection image reconstruction

$$f(x,y)=\int_{-\infty}^{\infty}\int_{-\infty}^{\infty}F(u,v)e^{j2\pi(ux+vy)}dudv \qquad (5\text{-}111)$$

Let $u=\omega\cos\theta,\ v=\omega\sin\theta,$ then $dudv=\omega d\omega d\theta$

$$f(x,y)=\int_{0}^{2\pi}\int_{0}^{\infty}F(\omega\cos\theta,\omega\sin\theta)e^{j2\pi\omega(x\cos\theta+y\sin\theta)}\omega d\omega d\theta \qquad (5\text{-}112)$$

$$f(x,y)=\int_{0}^{2\pi}\int_{0}^{\infty}G(\omega,\theta)e^{j2\pi\omega(x\cos\theta+y\sin\theta)}\omega d\omega d\theta \qquad (5\text{-}113)$$

Since $G(\omega,\theta+180^{\circ})=G(-\omega,\theta)$

$$f(x,y)=\int_{0}^{\pi}\int_{-\infty}^{\infty}|\omega|G(\omega,\theta)e^{j2\pi\omega(x\cos\theta+y\sin\theta)}\ d\omega\ d\theta \qquad (5\text{-}114)$$

$$f(x,y)=\int_{0}^{\pi}\left[\int_{-\infty}^{\infty}|\omega|G(\omega,\theta)e^{j2\pi\omega\rho}d\omega\right]_{\rho=x\cos\theta+y\sin\theta}d\theta \qquad (5\text{-}115)$$

$|\omega|$ is Ramp Filter

5.11 Image Reconstruction from Projections

5.11.5 Reconstruction Using Parallel-Beam Filtered Backprojections

- Hamming Window and Hann Window

$$h(\omega) = \begin{cases} c + (c-1)\cos\dfrac{2\pi\omega}{M-1} & 0 \le \omega \le (M\text{-}1) \\ 0 & \text{otherwise} \end{cases} \qquad (5\text{-}116)$$

For Hamming window, $c = 0.54$; for Hann window, $c = 0.5$

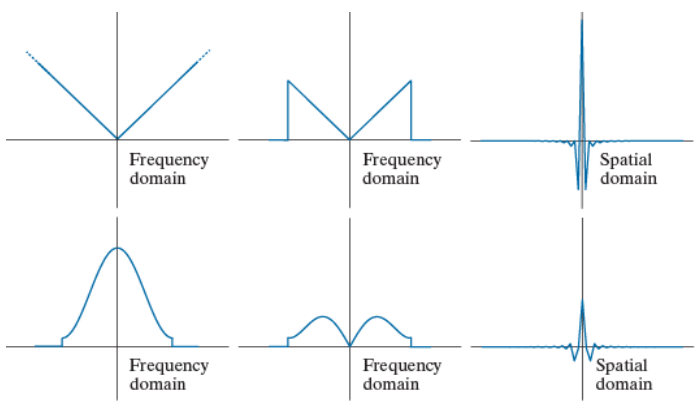

a b c
d e f

FIGURE 5.42 (a) Frequency domain ramp filter transfer function. (b) Function after band-limiting it with a box filter. (c) Spatial domain representation. (d) Hamming windowing function. (e) Windowed ramp filter, formed as the product of (b) and (d). (f) Spatial representation of the product. (Note the decrease in ringing.)

5.11 Image Reconstruction from Projections

5.11.5 Reconstruction Using Parallel-Beam Filtered Backprojections

- Steps of filtering backprojection to reconstruct an image
  1. Calculate the 1-D Fourier transform for each projection
  2. Multiply each Fourier transform by a filter function $|\omega|$, and this filter function has been multiplied by the appropriate window.
  3. 1-D Fourier inverse transform is performed on each filtered Fourier transform
  4. Accumulate (integrate) all 1-D Fourier inverse transforms obtained in the previous step

5.11 Image Reconstruction from Projections

5.11.5 Reconstruction Using Parallel-Beam Filtered Backprojections

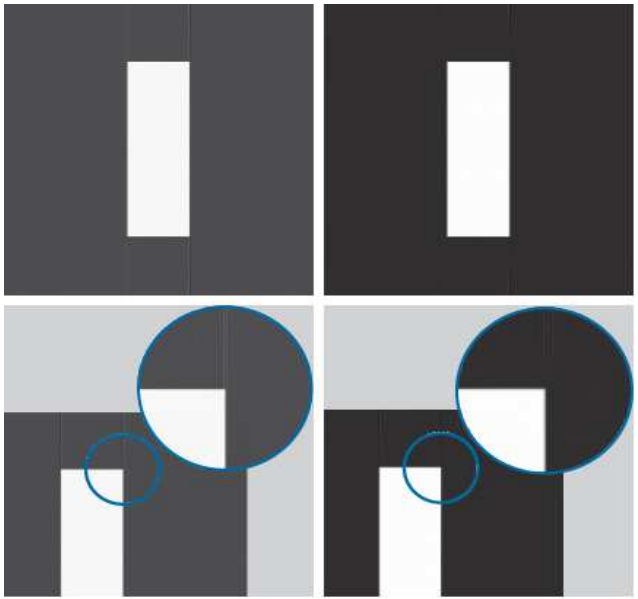

a b
c d

FIGURE 5.43 Filtered backprojections of the rectangle using (a) a ramp filter, and (b) a Hamming windowed ramp filter. The second row shows zoomed details of the images in the first row. Compare with Fig. 5.40(a).

5.11 Image Reconstruction from Projections

5.11.5 Reconstruction Using Parallel-Beam Filtered Backprojections

a b

FIGURE 5.44 Filtered backprojections of the head phantom using (a) a ramp filter, and (b) a Hamming windowed ramp filter. Compare with Fig. 5.40(b)

$$f(x,y) = \int_0^{\pi} \left[\int_{-\infty}^{\infty} |\omega| G(\omega,\theta) e^{j2\pi\omega\rho} d\omega \right]_{\rho = x\cos\theta + y\sin\theta} d\theta$$

$$= \int_0^{\pi} \left[s(\rho) \bigstar g(\rho,\theta) \right]_{\rho = x\cos\theta + y\sin\theta} d\theta \qquad (5\text{-}117)$$

$$= \int_0^{\pi} \left[\int_{-\infty}^{\infty} g(\rho,\theta) s(x\cos\theta + y\sin\theta - \rho)\, d\rho \right] d\theta$$

Individual backprojections at an angle θ can be obtained by convolving the corresponding projection, $g(\rho,\theta)$, and the inverse Fourier transform of the ramp filter, $s(\rho)$.

5.11 Image Reconstruction from Projections

5.11.5 Reconstruction Using Parallel-Beam Filtered Backprojections

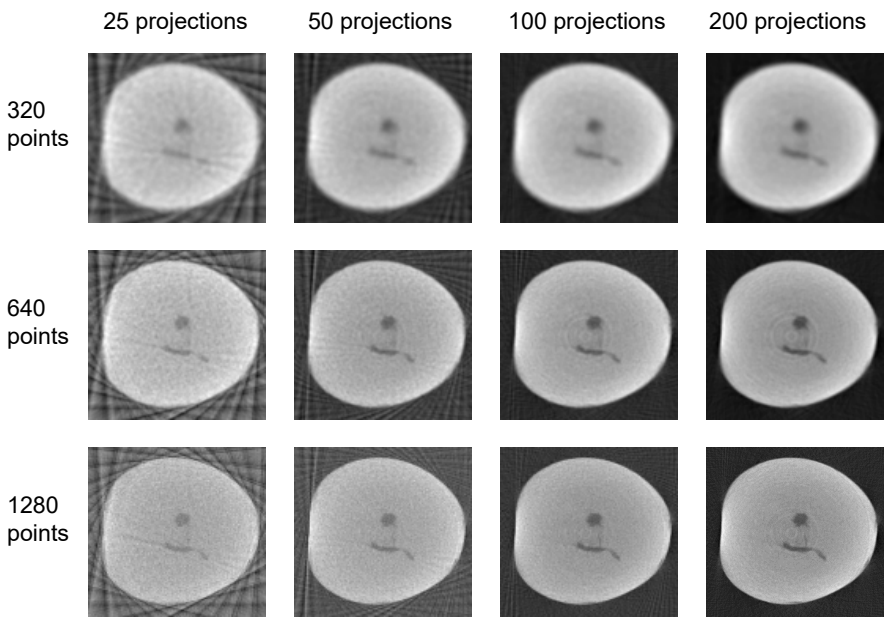

5.11 Image Reconstruction from Projections

5.11.5 Reconstruction Using Parallel-Beam Filtered Backprojections

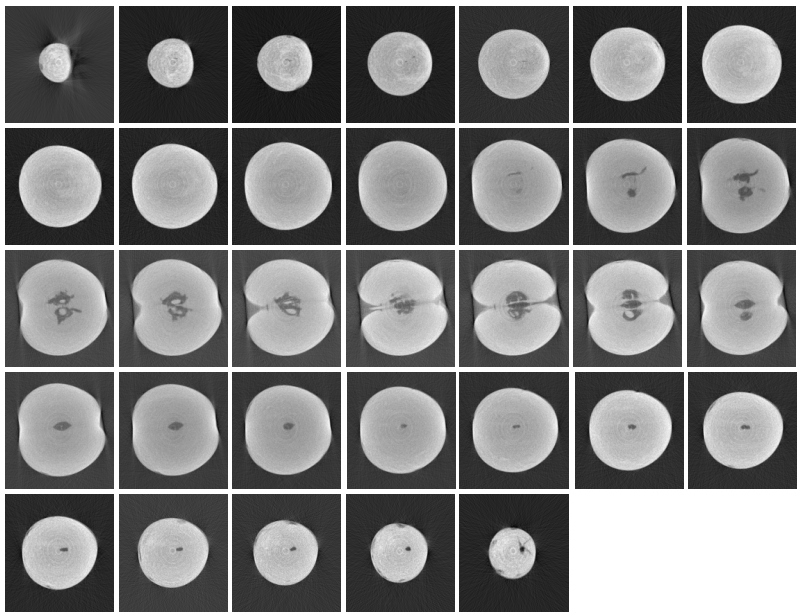

5.11 Image Reconstruction from Projections

5.11.5 Reconstruction Using Parallel-Beam Filtered Backprojections

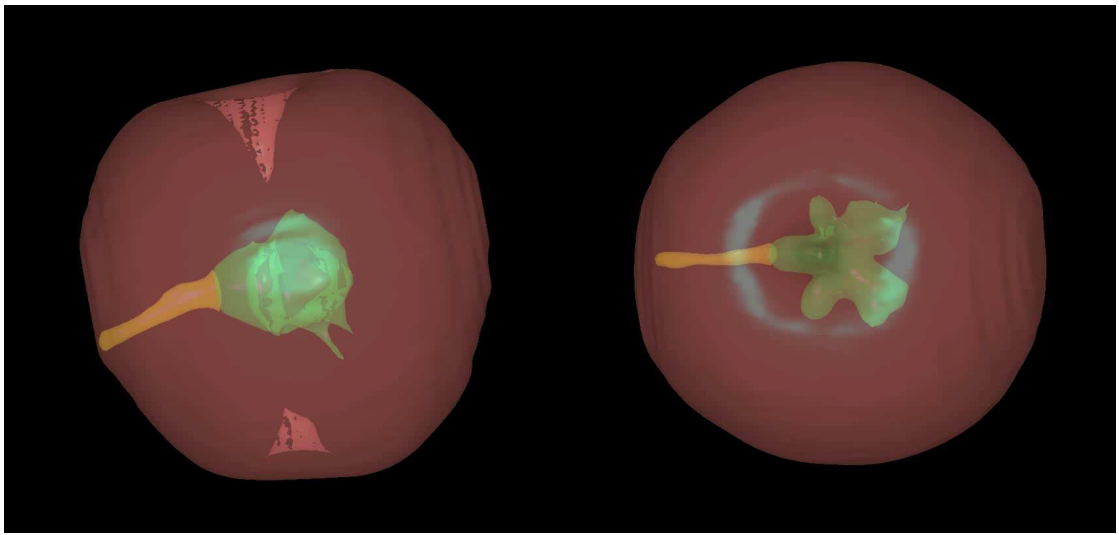

(a) (b)

APPLE

5.11 Image Reconstruction from Projections

5.11.6 Reconstruction Using Fan-Beam Filtered Backprojections

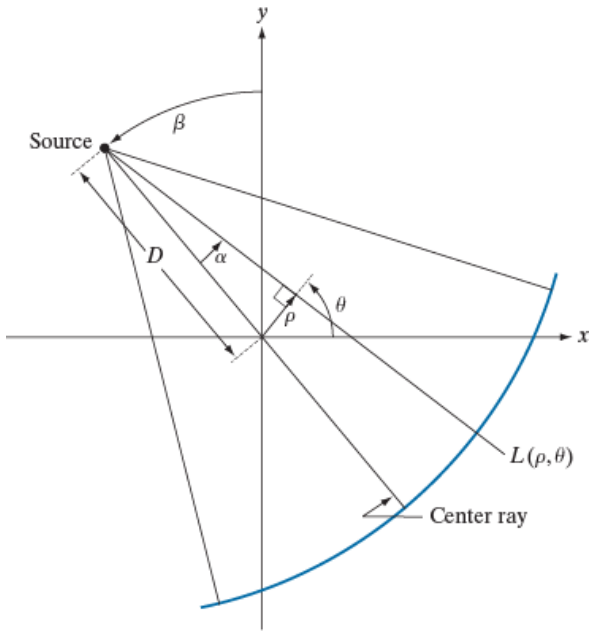

FIGURE 5.45
Basic fan-beam geometry. The line passing through the center of the source and the origin (assumed here to be the center of rotation of the source) is called the *center ray*.

5.11 Image Reconstruction from Projections

5.11.6 Reconstruction Using Fan-Beam Filtered Backprojections

- Derivation of convolution form

$$\theta = \beta + \alpha \qquad (5\text{-}118)$$

$$\rho = D\sin\alpha \qquad (5\text{-}119)$$

Suppose that we focus attention on objects that are encompassed within a circular area of radius T about the origin of the xy-plane

Then $g(\rho,\theta) = 0$ for $|\rho| > T$ and Eq.(5-117) becomes

$$f(x,y) = \frac{1}{2}\int_0^{2\pi}\int_{-T}^{T} g(\rho,\theta)s(x\cos\theta + y\sin\theta - \rho)d\rho d\theta \qquad (5\text{-}120)$$

Let $x = r\cos\phi,\ y = r\sin\phi$

$$x\cos\theta + y\sin\theta = r\cos\phi\cos\theta + r\sin\phi\sin\theta$$

$$= r\cos(\theta - \phi) \qquad (5\text{-}121)$$

So that Eq. (5-120) can be expressed as

$$f(x,y) = \frac{1}{2}\int_0^{2\pi}\int_{-T}^{T} g(\rho,\theta)s[r\cos(\theta - \phi) - \rho]d\rho d\theta \qquad (5\text{-}122)$$

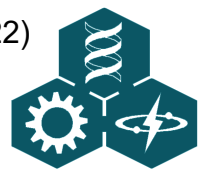

5.11 Image Reconstruction from Projections

5.11.6 Reconstruction Using Fan-Beam Filtered Backprojections

- Derivation of convolution form

In order to intergrate with respect to α and β, we use Eq. (5-118) and Eq. (5-119) for coordinate transformation:

$$f(r,\phi)=\frac{1}{2}\int_{-\alpha}^{2\pi-\alpha}\int_{\sin^{-1}(-T/D)}^{\sin^{-1}(T/D)} g(D\sin\alpha,\alpha+\beta)\, s[r\cos(\beta+\alpha-\phi)-D\sin\alpha]D\cos\alpha\, d\alpha\, d\beta \qquad (5\text{-}123)$$

$$f(r,\phi)=\frac{1}{2}\int_{0}^{2\pi}\int_{-\alpha_m}^{\alpha_m} p(\alpha,\beta)s[r\cos(\beta+\alpha-\phi)-D\sin\alpha]\, D\cos\alpha\, d\alpha\, d\beta \qquad (5\text{-}124)$$

This is the fundamental fan-beam reconstruction formula based on filtered backprojections

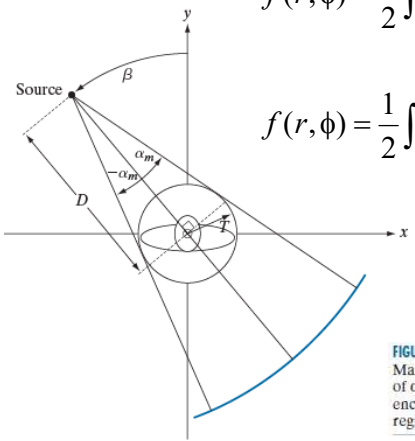

FIGURE 5.46
Maximum value of α needed to encompass a region of interest.

5.11 Image Reconstruction from Projections

5.11.6 Reconstruction Using Fan-Beam Filtered Backprojections

- Derivation of convolution form

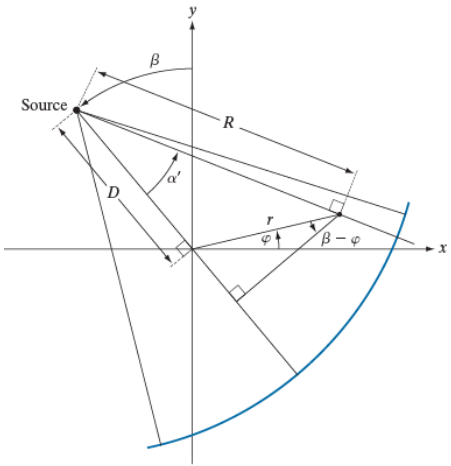

FIGURE 5.47 Polar representation of an arbitrary point on a ray of a fan beam.

Eq. (5-124) can be further manipulated in a more familiar convolution form:

$$r\cos(\beta+\alpha-\phi)-D\sin\alpha=R\sin(\alpha'-\alpha) \qquad (5\text{-}125)$$

$$f(r,\phi)=\frac{1}{2}\int_0^{2\pi}\int_{-\alpha_m}^{\alpha_m} p(\alpha,\beta)s[R\sin(\alpha'-\alpha)]D\cos\alpha\, d\alpha\, d\beta \qquad (5\text{-}126)$$

5.11 Image Reconstruction from Projections

5.11.6 Reconstruction Using Fan-Beam Filtered Backprojections

- Derivation of convolution form

$$s(R\sin\alpha) = \left(\frac{\alpha}{R\sin\alpha}\right)^2 s(\alpha) \qquad (5\text{-}127)$$

$$f(r,\phi) = \int_0^{2\pi} \frac{1}{R^2}\left[\int_{-\alpha_m}^{\alpha_m} q(\alpha,\beta)h(\alpha'-\alpha)]d\alpha\right]d\beta \qquad (5\text{-}128)$$

where

$$h(\alpha) = \frac{1}{2}\left(\frac{\alpha}{R\sin\alpha}\right)^2 s(\alpha) \qquad (5\text{-}129)$$

$$q(\alpha,\beta) = p(\alpha,\beta)D\cos\alpha \qquad (5\text{-}130)$$

5.11 Image Reconstruction from Projections

5.11.6 Reconstruction Using Fan-Beam Filtered Backprojections

- Derivation of convolution form

Instead of implementing Eq. (5-128) directly, an approach used often, particularly in software simulations, is to:

1. Use Eq. (5-127) and Eq. (5-128) to convert the geometry of the fan-beam projection into geometry of a parallel-beam projection
2. Use the parallel-beam reconstruction approach developed earlier.

An example is presented as follows:

$$p(\alpha,\beta) = g(\rho,\theta)$$
$$= g(D\sin\alpha, \alpha+\beta) \qquad (5\text{-}131)$$

We impose the restriction that

$$\Delta\beta = \Delta\alpha = \gamma \qquad (5\text{-}132)$$

Then $\beta = m\gamma$, $\alpha = n\gamma$, and we can write Eq. (5-131) as

$$p(n\gamma, m\gamma) = g[D\sin n\gamma, (m+n)\gamma] \qquad (5\text{-}133)$$

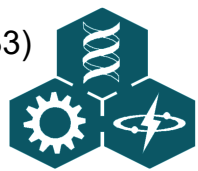

5.11 Image Reconstruction from Projections

5.11.6 Reconstruction Using Fan-Beam Filtered Backprojections

- Example

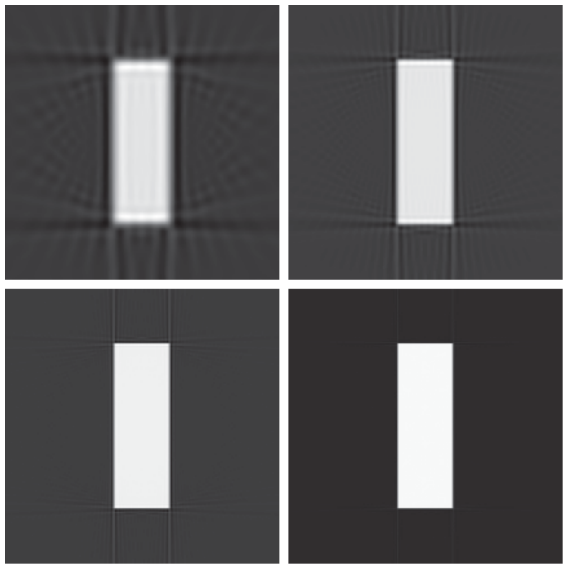

a b
c d

FIGURE 5.48
Reconstruction of the rectangle image from filtered fan backprojections. (a) 1° increments of α and β. (b) 0.5° increments. (c) 0.25° increments. (d) 0.125° increments. Compare (d) with Fig. 5.43(b).

5.11 Image Reconstruction from Projections

5.11.6 Reconstruction Using Fan-Beam Filtered Backprojections

- Example

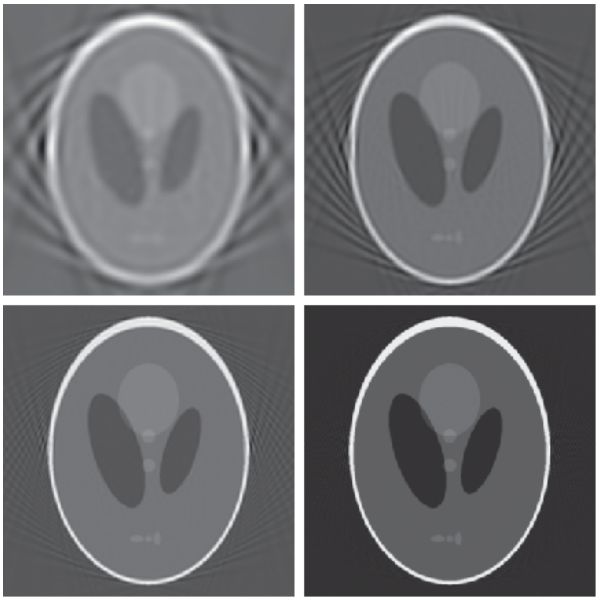

a b
c d

FIGURE 5.49
Reconstruction of the head phantom image from filtered fan backprojections. (a) 1° increments of α and β. (b) 0.5° increments. (c) 0.25° increments. (d) 0.125° increments. Compare (d) with Fig. 5.44(b).